A cockle-induced bioturbation model and its impact on sediment erodibility: A meta-analysis

Amélie Lehuen, Francis Orvain

Amélie Lehuen*[a], Francis Orvain[a]

[a] Biologie des Organismes et Ecosystèmes Aquatiques (BOREA) Université de Caen Normandie UNICAEN, Sorbonne Université, MNHN, UPMC Univ Paris 06, UA, CNRS 8067, IRD, Esplanade de la paix, F-14032 Caen, France

* Corresponding author : amelie.lehuen@gmail.com

A cockle-induced bioturbation model and its impact on sediment erodibility: A meta-analysis.

Abstract

Modelling the dynamics of an estuary and the evolution of its morphology requires a process-based description not only of the physical processes, but also of the influence of benthic fauna on sediment characteristics at ecosystem scale. A meta-analysis was tested as an approach for modelling the effect of bioturbation exerted by the cockle *Cerastoderma edule* on sediment erodibility. Six different erosion flume datasets were collected to ensure a broad range of experimental conditions including bed shear stress, population characteristics, and sediment composition. First, a model was built to describe the biogenic fluff layer created by *C. edule* activity in relation to (i) bioturbation activity using the population metabolic rate [$mW.m^{-2}$] as a proxy for faunal metabolic energy, and (ii) the silt content [%] of the sediment. Second, different erosion models were compared by testing parameterization steps incorporating both erosion of the fluff layer and/or mass erosion of the sediment bed. Structural differences in the flumes and in the preparation of samples in the six different datasets makes it difficult to propose a single model that satisfactorily simulates all the data and encompasses both types of subsequent erosion, that of the fluff layer and that of the underlying consolidated bed. However, a generic model is proposed for the surficial fluff layer erosion covering a moderate range of bed shear stress (<1 Pa). This study shows that including several datasets covering a wide range of environmental conditions is a key to the robustness of this model, and that new insights can be gained by integrating the complexity of sediment features. We expect that this two-part model can be used in broad contexts

in terms of cockle populations, estuarine habitats, and climatic conditions and can combined with various hydro-morpho-sedimentary models that include these biological effects.

Highlights

- 6 erodibility studies were used to parametrize a generic model of the bioturbation effect of the cockle Cerastoderma edule.
- A model of the fluff layer made by cockles' bioturbation is proposed using the metabolic rate and the silt content.
- This model simulates sediment resuspension at moderate bed shear stress, whatever flume, population or sediment.
- It is more difficult to fit a model reliable for simulating sediment resuspension at high bed shear stress.

Keywords

Model, *Cerastoderma edule*, erosion, erodibility, bioturbation, metabolic rate, sediment transport, hydrosedimentary processes

Graphical abstract

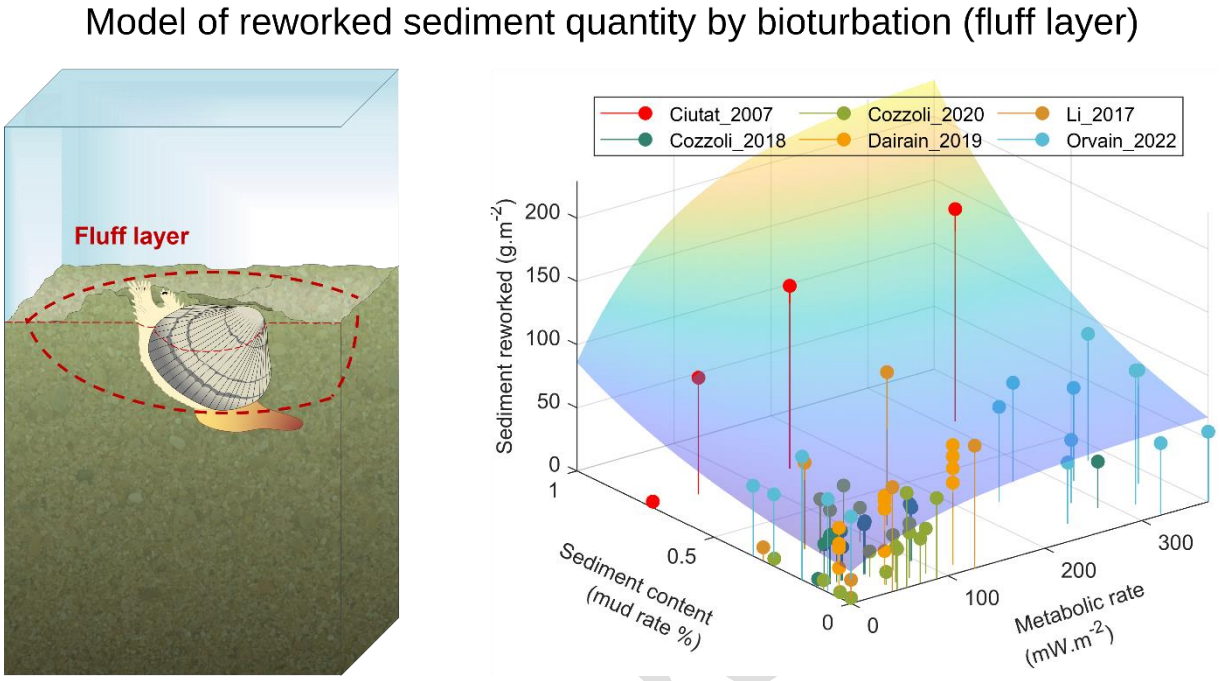

Manuscript

1 Introduction

An estuary is an ecosystem at the interface of a river and the ocean, an ecotone through which energy and material flows both upstream and downstream and where a haline front creates a mobile turbidity maximum that shifts with the tide. The extent of the tidal regime defines the range of physico-chemical parameters of the estuary (salinity, flooding time, sediment texture, etc.), which intrinsically define different habitats such as salt marshes, sand banks, and intertidal mudflats (Dronkers and van den Berg, 2023). This mosaic of habitats is very diverse and highly productive, and provides a variety of ecosystem services including natural resources, possible recreational activities, as well as regulation services including nutrient transfer, eutrophication, coastline protection, reducing flood risks, greenhouse gas sequestration, cultural services, and other socio-economic benefits (Barbier et al., 2011).

Although the physical phenomena that drive sediment transport in an estuary still need to be refined, some hydro-morpho-sedimentary (HMS) models are well established and are increasingly accurate and process based (Baas et al., 2013; Diaz et al., 2020; Grabowski et al., 2011; Grasso et al., 2015; Le Hir et al., 2011). HMS factors are physical habitat-defining parameters, on which lifetraits and lifespans of biological communities fully depend (Herman et al., 2001; Ysebaert and Herman, 2002). In particular, sediment properties and hydrological parameters have direct impacts on the activity and spatial distribution of macrozoobenthos, with sediment pools representing food sources, habitats, refuges and nurseries. The grain size distribution of the sediment, represented by the median grain size and the silt content (< 63 µm), play a particular role in explaining variations in macrozoobenthic communities (Degraer et al., 2006; Thrush et al., 2005).

Conversely, benthic bioturbators are ecosystem engineering species (Jones et al., 1994), which have the ability to actively modify their immediate environment by moving particles, either by foraging for food or by other behaviours involving mobility. Many HMS models of sediment transport neglect the relevance of biological factors such as bioturbation in the control of sediment transport, in particular sediment erosion even though it has been demonstrated via two main approaches. On one hand, a reductionist laboratory approach, studies using process-based models of sediment transport, with controlled abiotic parameters, isolated bioturbating species and a design with few factors (Cozzoli et al., 2020; Dairain et al., 2020b; Le Hir et al., 2007; Orvain, 2005; Orvain et al., 2012; Paarlberg et al., 2005; van Prooijen et al., 2011; Wood and Widdows, 2002). On the other hand, a global *in-situ* approach can be applied, integrating the complete structure of the sediment, the presence of micro-algae and the biological community present, often in order to isolate the most contributory species or to focus on one species in particular (Harris et al., 2015; Joensuu et al., 2018; Li et al., 2021; Needham et al., 2013, 2013; Shi et al., 2020).

Depending on the behaviour of species, different processes take place which can also be expressed at different magnitudes depending on the environmental conditions (Andersen et al., 2002; Orvain et al., 2007; Widdows and Brinsley, 2002). Many flume experiments have been conducted to evaluate the impact of different species on sediment resuspension (e.g. Andersen et al., 2010; Orvain et al., 2003; Widdows et al., 1998). The variety of sediments, temperatures and feeding conditions, either circumstantial or experimental factors, have a wide range of results (Amos et al., 1992; Andersen, 2001; Soissons et al., 2019; Widdows et al., 1998). The list of environmental factors likely to modify the extent

of sediment bioturbation and its impact on erodibility includes: (i) physical factors such as the water content of the sediment, the emersion time (Orvain et al., 2003), the sediment consolidation status (Orvain et al., 2003; Orvain and Sauriau, 2002), the sediment grain size composition (Ubertini et al., 2015) and (ii) the biological variables that reflect interspecific interactions, such as the biomass of microphytobenthic chl *a* as food resources (Andersen et al., 2010; Dairain et al., 2020b; Orvain et al., 2004) or contamination by parasitic pathogens (Dairain et al., 2020a).

The common cockle *Cerastoderma edule* (Linnaeus, 1758) has been widely studied as a destabilising biodiffusor living in rather transitional areas of the foreshore and subject to medium currents (Cozzoli et al., 2014; Herman et al., 1999), typically marine salinity values (> 30 PSU) and that prefers fine sands (Cozzoli et al., 2014; Ubertini et al., 2012). Its broad distribution around the Atlantic (Hayward and Ryland, 1995) and the economic interest for fishermen has made it a good target model organism to investigate flow/sediment/organism interactions (Eriksson et al., 2017; Soissons et al., 2019).

This bivalve *C. edule* causes surface reworking of the sediment and sediment erosion by valve movements and feeding. These movements create a layer with a low erosion threshold called the sediment fluff layer (Ciutat et al., 2007; Cozzoli et al., 2020, 2019; Dairain et al., 2020b; Orvain et al., 2003). Conversely, it can have a stabilising effect on sandy sediments by promoting biodeposition linked to filtration feeding and can increase the silt content by incorporating particles in the top centimetres of sediment (Donadi et al., 2014; Li et al., 2017; Soissons et al., 2019). Bio-stabilisation has also been reported to promote colonisation by microphytobenthos, which has an additional stabilising effect (Andersen et al., 2010; Rakotomalala et al., 2015; Sutherland et al., 1998).

Erosion studies generally measure the effect of biomass or of the density *of C. edule* on sediment resuspension. However, the body size of each individual cockle is also an important factor, because the roughness created by the presence of the shell disrupts the surface of the sediment (Dairain et al., 2020b). Sediment reworking is also linked to the behavioural activity of cockles (valve movement, feeding, burrowing, etc.) which can be affected by physical factors such as temperature and physiological metabolism but which can be weakened by pathogen infection (Dairain et al., 2020a; Zhou et al., 2022).

Metabolic rate appears to be a good proxy to assess the activity of an individual (Brown et al., 2004). The mass specific respiration rate (MSR) developed by Brey (Brey, 2010) firstly to assess respiration at

the level of a population or community, includes population density, mean body size and temperature. Several studies have used the metabolic rate specifically to assess sediment erodibility under the influence of bioturbation (Cozzoli et al., 2020, 2019, 2018), by converting the biomass and density of a biota into an energy flux per unit surface area.

In this study, we revisited existing datasets from laboratory flume experiments though a meta-analysis with two main goals: (1) to aggregate different experimental conditions to extend the set of biological conditions (biomass, density and individual body size) and to explore the interacting role of sediment characteristics, in particular silt content, which mediates the influence of the bioturbator on bed erodibility; (2) to use the MSR rate to characterise the biological factor, to reflect the activity of the organism that results in bioturbation at different temperatures, thus seasonality. Modelling bioturbation processes on the basis of these parameters enables them to be integrated into the description of hydrodynamic sediment transport processes. In particular, by reflecting two aspects of biological activity - the variation of bioturbation activity with season and sediment type - this model allows application on a wider temporal and spatial scale, an element missing for the HMS modelling approach, which prevents from assessing the long-term impact of bioturbation on coastal or estuarine morphology.

2 Materials and methods

All data processing was conducted in R version 4.2.2 (2022-10-31 ucrt) and Matlab 2021a. Significance levels are $p < .0001$ with "****", $p < .001$ with "***", $p < .01$ with "**", $p < .05$ with "*".

2.1 Metabolic rate

The metabolic rate was estimated in this study by the mass specific respiration rate (MSR) of aquatic invertebrates developed by Brey (Brey, 2010), by using a spreadsheet tool that implements an artificial neural network. The spreadsheet requires as variables: (1) individual body mass in J, (2) temperature in K, (3) depth in the water column, (4) taxonomic definition, (5) mobility mode (sessile, crawler, elective or permanent swimmer/floater), (6) alimentation mode (carnivorous versus other modes), (7) type of vision ('yes or no' defined as possession of image-forming eyes *sensu* (Seibel and Drazen, 2007), i.e. a better optical sense than merely being able to distinguish light from dark), and (8) the starved state of the animal (yes or no). The bivalve *C. edule* is classified as Mollusca 1, is sessile, not carnivorous and has no vision.

MSR was calculated using the average energy density 21.4469 J.mgAFDW^{-1} (Brey et al., 2010), a depth of 1 m for intertidal species, and by default not starved. MSR was converted from [J/J/day] to [mW.ind^{-1}]. The MSRtot is defined (MSR*Density, [mW.m^{-2}]), as the total metabolic energy of the sample.

2.2 Erosion data

Erosion data were collected from six studies of *C. edule* performed in different experimental conditions with different recirculating flumes.

The first dataset came from an experiment that used an annular flume (Ciutat et al., 2007). The muddy sediment (72.3 % <63 µm), sampled from the Tamar estuary (southwest England), was maintained as found in the field and inserted directly into the flume. All measurements were performed at 15 °C in a climate-controlled room, with an alternating day/night regime, and the fauna was maintained for 24 h in the flume and then for 24 h in sinusoidal cycles of current velocity to mimic tidal cycles before erosion was measured. Fed with phytoplankton (*Isochrysis galbana*) the fauna was set up at 3 density levels and a control (47.06 to 311.76 ind.m^{-2}; 25.41 to 168.35 gAFDW.m^{-2}). Current velocity ranged from 5 to 50 cm.s^{-1} in 12 steps each lasting 15 to 50 min. The set comprised 4 runs, including 1 control run.

The second study used an annular flume (Cozzoli et al., 2018). Only data concerning the bivalve *C. edule* was selected. The muddy sand sediment (12 % < 63µm) was defaunated, homogenised and wetted so it would settle and consolidate in the flume. The flumes were placed in a climate-controlled room at 18 °C, filled with filtered marine water, and the fauna bioturbation time was 48 h. The experimental setup crossed 3 individual body sizes and 4 densities (3 in the case of large bivalves; 12.74 to 382.17 ind.m^{-2}; 1.03 to 117.72 gAFDW.m^{-2}). Current velocity ranged from 10 to 35 cm.s^{-1} in 6 steps each lasting 20 min. Each combination was performed with 2 replicates and one control prior to each body size, giving a total of 28 runs including 6 control runs.

The third dataset was taken from a study also made using an annular flume (Cozzoli et al., 2020). The sediment parameter comprised 4 percentage silt contents (0-28 % <63 µm), obtained by mixing defaunated, homogenised and wetted sediment that was allowed to settle and consolidate in the flume. The flumes were placed in a climate-controlled room at 18 °C, filled with filtered marine water, and the fauna bioturbation time was 48 h. The fauna factor comprised 4 combinations of sizes of individual

cockles and density (33.16 to 530.52 ind.m^{-2}) to maintain the same total biomass (19.1 gAFDW.m^{-2}). Current velocity ranged from 5 to 30 cm.s^{-1} in 7 steps each lasting 20 min. Each combination was performed with two replicates and a control prior to each run, giving a total of 28 runs performed, plus 32 controls.

The fourth dataset was extracted from an experiment using a one-way flume, ERIS (Dairain et al., 2020b). The slightly muddy sand sediment (4.4% <63 µm) was obtained by mixing defaunated, homogenised and concentrated sediments, and filled in cores. The mesocosm was filled with filtered marine water at a field temperature of 12 °C with a semi-diurnal tidal cycle (one diurnal emersion phase), and the fauna bioturbation time was 6 days. The experimental design had 4 factorial parameters: mesocom with or without phytoplankton (*Isochrysis galbana*), with or without microphytobenthos (MPB) enrichment, 2 physiological states of fauna: parasitised and unparasitised, and 2 density levels (314.38 to 785.95 ind.m^{-2}; 22.02 to 55.05 gAFDW.m^{-2}) plus a control. Current velocity ranged from 0 to 72.5 cm.s^{-1} in 20 steps each lasting 5 min. Each combination was made with 3 replicates, giving a total of 36 runs, including 12 controls.

The fifth dataset was collected from an experiment using an annular flume (Li et al., 2017). The sediment had 2 levels of silt content (0 % and 32 % <63 µm), obtained by mixing defaunated, homogenised and wetted sediment poured into the flume and allowed to consolidate. The flumes were placed in a climate room at 15 °C, filled with filtered marine water, and the fauna bioturbation time was 48 h. The fauna had 2 density levels (228 to 686 ind.m^{-2}; 14.1 to 42.24 gAFDW.m^{-2}). Current velocity ranged from 5 to 40 cm.s^{-1} in 8 steps each lasting 20 min. The results are the average of 3 replicates of each run and 3 controls for each density, giving a total of 6 mean runs, including 2 controls. These data were retrieved by graphic analysis using the Matlab “digitize” function (Sanchez, 2006).

The sixth dataset originated from an experiment made by F. Orvain (2022, unpublished) using a one-way flume, ERIS. The sediment parameter had 5 levels of silt content (0 to 36 % <63 µm), obtained by mixing defaunated, homogenised sediments, and filled in cores. The fauna was settled in cores and measurements were made immediately after in filtered sea water at 14.96±1.27°C (bioturbation time was 0 day). The fauna factor was 2 combinations of individual size (juveniles and adults) and densities to keep the same total biomass (157.19 to 471.57 ind.m^{-2}; 33.2 to 36 gAFDW.m^{-2}). Current velocity ranged from 0 to 83 cm.s^{-1} in 14 steps each lasting 5-8 min. Each combination was made with 1 replicate, giving a total of 15 runs, including 5 controls.

The dataset that combined the experimental results of the 6 aforementioned studies consisted of 149 time series, 91 with fauna, and 58 control experiments. The dataset contained two types of BSS ranges linked to the two types of flumes, with ERIS (Dairain_2019 and Orvain_2022) reaching values up to 10 times higher than annular flumes. In terms of erosion measurement time, the Ciutat_2007 experiments lasted around 8 h, those of Cozzoli_2018, 2020, and Li_2017 lasted 2 h, and those of Dairain_2019 and Orvain_2022 lasted 1h30. Only the Ciutat_2007 set had a high silt content (72%), the other sets were all in the same range, from 0 to 36%, for a total of 12 levels. The biological ranges were fairly well distributed, MSRtot varied on 33 levels, from 6.23 to 368.33 $mW.m^{-2}$, on 3 temperature levels, from 12 to 18°C. The bioturbation duration prior to erosion measurement was highly dependant of the experiment from none in Orvain_2022 to 6 days in Dairain_2019 (Table 1, Figure 1).

Table 1. Characteristics of the experimental set-up for each dataset. BSS: bed shear stress.

	Cuitat _2007	**Cozzoli _2018**	**Cozzoli _2020**	**Dairain _2019**	**Li_2017**	**Orvain _2022**
Type of flume	Annular	Annular	Annular	One way flume	Annular	One way flume
Current speed ($cm.s^{-1}$)	5 – 50	10 – 35	5 – 30	0 – 72.5	5 – 40	0 – 83
BSS (Pa) max	0.370	0.249	0.183	1.65	0.326	2.29
Sample surface (m^2)	0.17	0.157	0.157	0.0016	0.157	0.0016
Water volume (L)	46	31.4	31.4	21	31.4	21
Plateaus length (min)	15-50	20	20	5	20	5-8
Plateaus nb	12	6	7	20	8	14
Nb records	7,289	6,686	13,768	29,757	1,245	16,836
Temperature (°C)	15	18	18	12	15	15
Silt content (%)	72.3	12	0 – 28	4.4	0 & 32	0 – 36
Sediment preparation	Natural	Decanted	Decanted	Moulded	Decanted	Moulded
Bioturbation time	24 h	48 h	48 h	6 days	48 h	0 h
Biological density ($ind.m^{-2}$)	47.1 – 311.8	12.7 – 382,2	33.2 – 530.5	314.4 – 786	228 – 686	157.2 – 471.6
Biological biomass ($gAFDW.m^{-2}$)	211.8 – 1402.9	1 – 117.7	19.1	22 – 55.1	14,1 – 42.2	33.2 – 36

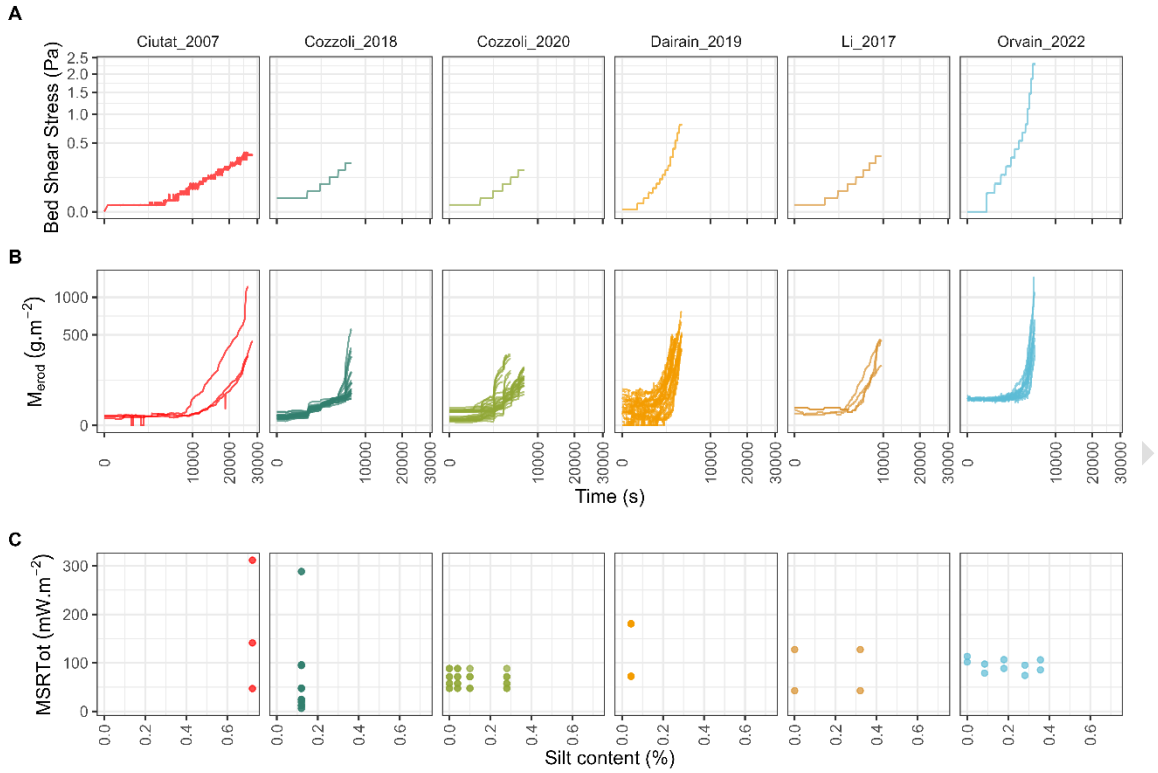

Figure 1. A: Bed sheer stress (BSS [Pa]) time scheme for each experiment, B: Resuspended mass (M_{erod} [g.m^{-2}]) versus time for each experiment and C: the metabolic rate calculated (MSRTot [mW.m^{-2}]) versus the sediment silt content [%] for each experiment.

2.3 Data treatment

The bed shear stress (BSS or τ [Pa]) for every run of each study was determined using their respective published estimates (Figure 1), and each turbidity measurement was converted into Resuspended mass calculated on the sample surface, M_{erod} [g.m^{-2}]. Every current step was defined, and fluff or mass erosion steps were identified visually. Every step was summarised by its mean hydrological conditions, and the 95th centile of the M_{erod}. The Q_{fluff_obs} was determined as the 95th centile of M_{erod} at the last fluff step before mass erosion became visible (Figure 2). The critical τ_{mass} [Pa] was calculated as the intercept of the best linear regression between U* and M_{erod} among mass steps as $M_{erod} = aU* + b$ thus $U* = -b/a$ with M_{erod} = 0.

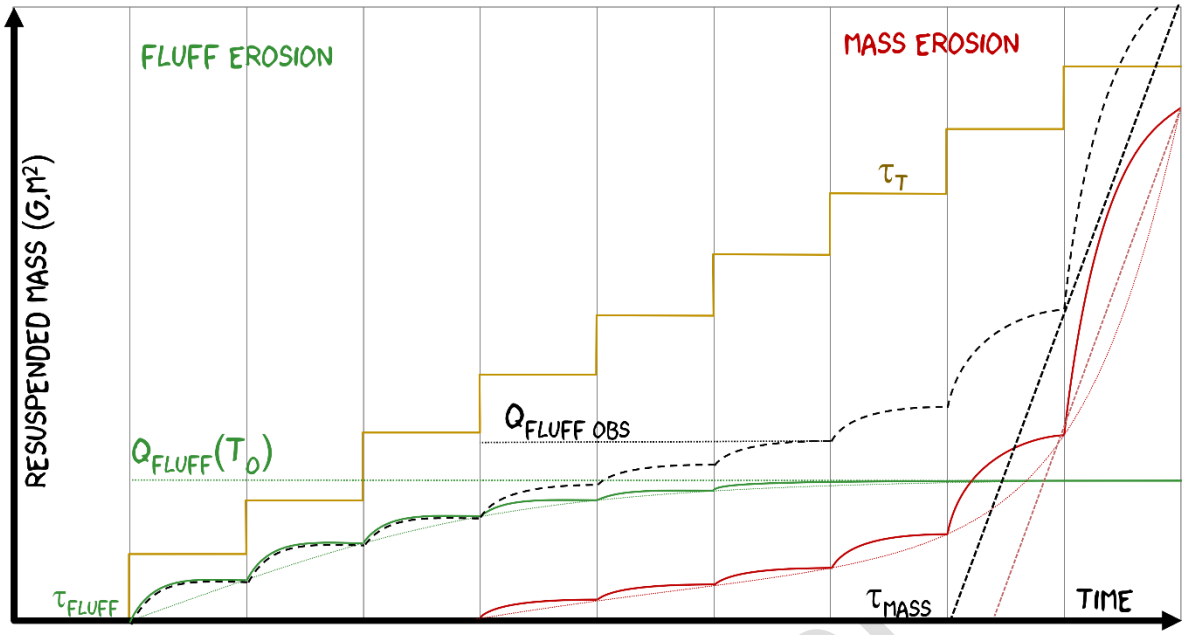

Figure 2. Sketch of erosion processes in the fluff layer erosion (green line), mass erosion (solid red line) and the parameters used. The dashed black line represents the addition of the two processes, the M_{erod} measured in the experiment. The straight dashed black line represents the linear regression of the mass erosion steps that determined the critical mass erosion threshold (τ_{mass} [Pa]).

2.4 Model building

2.4.1 Erosion model

The model erosion was based on several works including two by Orvain et al. (2003, 2012) that consider the erosion flux as the result of three processes (Equation 1).

Equation 1 $$\frac{dM_{erod}}{dt} = E_{fluff} + E_{mass} - D$$

where E_{fluff} is the fluff erosion rate, E_{mass} is the mass erosion rate and D the deposition flux, all [g.m^{-2}.s^{-1}]. For this study, we did not use the deposition flux for process simplification, the measured M_{erod} were considered as the result of the equilibrium between resuspension and deposition. The fluff erosion rate was based on Orvain's model development (Orvain et al., 2003) and expressed as Equation 2.

Equation 2 $$E_{fluff}(t) = \alpha . Q_{fluff}(t - dt) . \left(\frac{\tau_t}{\tau_{fluff}(t)} - 1\right) + o \; and \; E_{fluff} = 0 \; if \; \tau_t < \tau_{fluff}$$

where α is a kinetic erosion coefficient [s^{-1}] integrating the Q_{fluff} erodible amount of sediment, which varies in dt. The parameter τ_{fluff} [Pa] represents the BSS threshold (critical τ) when fluff erosion starts, known to be at low level. τ_t [Pa] is the dynamic BSS, the physical forcing variable that was applied on the sample at time t [s]. $Q_{fluff}(t\text{-}dt)$ is the remaining quantity of fluff layer (result of faunal activity reworking

the sediment) for the previous time interval. It was assumed that the amount of M_{erod} just before mass erosion (Q_{fluff_obs}) was a good proxy for the quantity of fluff layer generated on the sample before erosion began, called $Q_{fluff}(t0)$ [g.m^{-2}] (Figure 2). We assumed that $Q_{fluff}(t0)$ can be expressed as a function of biological and sediment factors (Equation 3).

Equation 3 $Q_{fluff}(t_0) \sim BioFact * SedFact$

where $BioFact$ is MSRTot [mW.m^{-2}], $SedFact$ stands for the silt content [%]. The biological part of this equation was chosen as a von Bertalanffy function, as its adequacy has been demonstrated in several studies describing this kind of process for other bioturbators like the gastropod *Peringia ulvae* or the bivalve *Macoma balthica* (Orvain and Sauriau, 2002; van Prooijen et al., 2011; Willows et al., 1998). For cockles it was used in models that specifically simulate microphytobenthos resuspension (Rakotomalala et al., 2015). In the latter study, the best minimised function was linear, as was the case for another bivalve, *Scrobicularia plana* (Orvain, 2005). Adding a sediment component to the model required exploring various mathematical functions without an *a-priori* (linear, von Bertalanffy) so as to adjust the quantity of sediment contained in an easily eroded fluff layer, and the dependence of this variable (Qfluff) on abiotic factors ($\mathrm{SedFact}$) (Supplementary Data 2.4.1).

The mass erosion rate is the expression of bed load erosion, as described in previous studies e.g. (Orvain et al., 2012), in line with the Partheniades formula for cohesive beds (Partheniades, 1965) (Equation 4).

Equation 4 $E_{mass}(t) = E_0 \cdot \left(\frac{\tau_t}{\tau_{mass}} - 1\right)$ and $E_{mass} = 0$ if $\tau_t < \tau_{mass}$

where E_0 is the erosion rate [g.m^{-2}.s^{-1}], τ_{mass} [Pa] represents the BSS threshold (critical τ) when mass erosion starts, and τ_t [Pa] the BSS applied to the sample at time t [s]. E_0 was made to vary as a function of biological factors and optionally as a function of the sedimentary factor (Equation 5, Supp Data 2.4.1).

Equation 5 $E_0 \sim E_{0\,ab} * BioFact\ (* SedFact)$

where E_{0ab} is the abiotic erosion rate [g.m^{-2}.s^{-1}], a function of sediment conditions, which was then modulated by biological conditions. In the same way, τ_{mass} is expressed as an abiotic $\tau_{mass0ab}$ potentially modified by biological factors and optionally by sedimentary factors (Equation 6, Supp Data 2.4.1).

Equation 6 $\tau_{mass} \sim \tau_{mass0ab} * BioFact \ (* SedFact)$

2.4.2 Model adjustment

The model was adjusted using the Simplex method in Matlab by minimising the ordinary least squares criterion (Sum of Squares Error). The model adjustment minimisation was made by the Matlab function fminsearchbnd (D'Errico, 2006), the boundaries being defined to ensure a realistic outcome for each parameter. The initial conditions for solving the fminsearch were optimised by using combinations of several values of each adjusted parameter. The adjustments to the model were made in five steps (Figure 3):

I. **Creation of the fluff layer**: This modelled process describes the biological effect of sediment reworking prior to erosion through the creation of an easily eroded fluff layer, due to the activity of surface fauna. $Q_{fluff}(t0)$ was **globally** adjusted (all observations fitted together) (Equation 3) based on Q_{fluff_obs} extracted from all the runs (Figure 2). The model with the best fit was selected by comparing 6 mathematical functions (Supp Data 2.4.1).

II. **Abiotic sediment erodibility: control mass erosion**: This model made it possible to calibrate differences in sediment properties linked to their content, preparation, and the experimental set up. Controls from all studies were selected and grouped **in series of sediment types** (including phytoplankton & MPB conditions for Dairain_2019, independently of the biological conditions, i.e. a total of 17 different adjustments). Each pool was adjusted on mass erosion parameters (Equation 4). Each adjustment parameter (E_{0ab} and $\tau_{mass0ab}$) was then associated with its corresponding biological run.

III. **Individual fluff & mass erosion**: This adjustment enabled us to determine whether combining the two types of erosion processes would improve model performance. The comparison of **individual** adjustments (grouped in replicates: the same conditions for sediment and fauna, a total of 68 different adjustments) using (i) the fluff equation (Equation 2), (ii) the mass equation (Equation 4), (iii) the fluff and mass equations combined (Equation 2 & Equation 4: Equation 1). These adjustments used the Qfluff(t0) (**I.**) and the control (**II.**) adjustment parameters as fixed parameters.

IV. **Sediment type, fluff & mass erosion**: The aim of this model was to fit the data more globally by grouping them according to the type of sediment, to only evaluate the capacity of the biological factor to account for the effects of bioturbation. Adjustments were made with fluff

and mass combined (Equation 2 & Equation 4: Equation 1) **per series of sediment types** using model parameters **I.** and **II.** as fixed parameters. The mass parameters were adjusted taking the fauna into account with Equation 5 and Equation 6.

V. **Global fluff & mass erosion**: This trial evaluated how the erosion processes can be fitted in a more global model by assuming that the mass erosion related to sediment variability is accounted for in the control **II.** parameters**.** The effects of bioturbation on mass erosion were thus generalised to all the runs. The mass parameters were adjusted by taking the fauna into account with Equation 5 and Equation 6. The **global** adjustments made with the fluff and mass combined (Equation 2 & Equation 4: Equation 1) were compared with those made with fluff erosion **on fluff steps** (Equation 2) using the **I.** and **II.** parameters as fixed parameters.

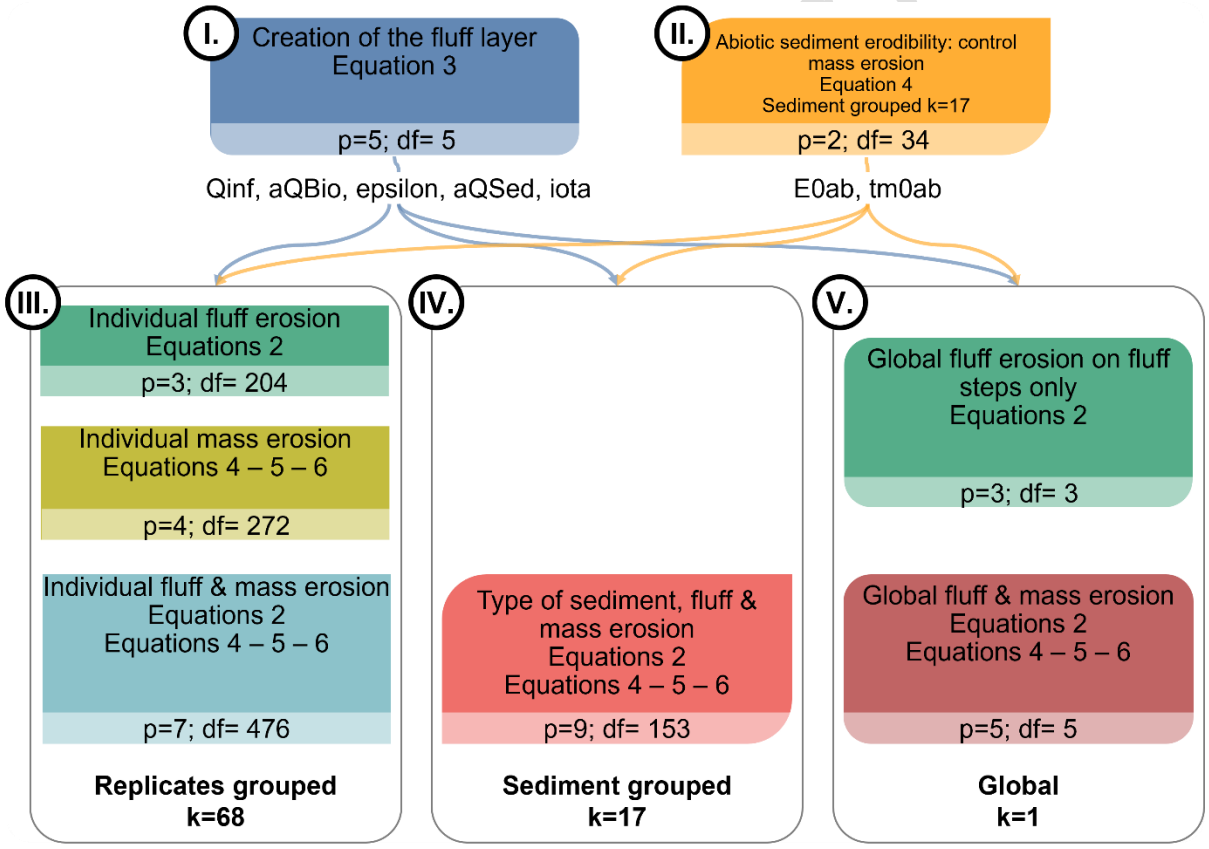

*Figure 3. Scheme of the adjustments made, p is the number of parameters, k the number of sub-groups, and df represents the degree of freedom as p*k.*

2.4.3 Model validation

The models were evaluated with the help of graphic visualisation and compared using model validation indexes calculated on the y = x relationship (diagonal) between the observed and modelled data.

The root mean squared error (RMSE) represents the standard deviation of the residuals, equivalent to σ when the estimator is unbiased. This criterion defines the extent of data scattering around the regression line. This non-standardised index is equivalent to its standardised counterpart R^2. Expressed in the same units as the response variable, this index can be normalised (nRMSE) with respect to the range of the response variable, which makes it possible to compare models of different datasets. The lowest RMSE indicates the best fit, but for an equivalent reading such as R^2, nRMSE is transformed as 1-nRMSE, hence the closer to 1 the better.

The Akaike information criterion (AIC), (Akaike, 1974) makes it possible to compare models with different numbers of parameters, i.e. to use as few parameters as necessary, the smaller AIC the better the fit. AICc is a second-order (or small sample) AIC with a correction for small sample size. The Bayesian Information Criterion (BIC) is interpreted as the AIC, with a higher penalty given to the number of parameters.

When necessary, post-hoc tests were performed on the observed and predicted data to assess the quality of the selected model: a Durbin-Watson test was used to evaluate the autocorrelation of residuals, which ranged from zero to four, where a value of 2.0 indicates zero autocorrelation. Values below 2.0 indicate a positive autocorrelation, and values above 2.0 a negative autocorrelation. Second, the Harrison-McCabe statistic was used to check whether the residuals were homoscedastic or heteroscedastic.

3 Results

High resolution figures showing the main results and complementary figures are in the supplementary data file, model result parameters Supplementary Table 3.A, and validation scores in Table 2 and in Supp. Table 3.B.

3.1 Model pre-adjustments

3.1.1 Creation of the fluff layer (I.)

The model was selected by analysing the model validation indexes, with nRMSE=0.806 (Figure 4, modelled-observed plot in Supp. Fig 3. B). The equation with coefficient values obtained by fitting methods, includes two terms (in brackets): a biotic one related to metabolism and an abiotic one that varies with the silt content of the sediment.

$$Q_{fluff}(t_0) = \left[Q_{inf}.\left(1 - e^{(-a_{Bio}.\mathrm{MSRtot})}\right) + \varepsilon\right].\left[\left(e^{(a_{Sed}.\%Silt)}\right) + \iota\right]$$

with $Q_{inf} = 20.163$; $a_{Bio} = 0.01$; $\varepsilon = 11.837$; $a_{Sed} = 1.815$; $\iota = 1.12$

Overall, the model tended to slightly underestimate the quantity of eroded fluff layer (Figure 4). The bioturbation model went up to 200g.m^{-2}, representing eroded material up to 1 mm in height assuming a sediment concentration of 200kg.m^{-3}. This order of magnitude therefore seems realistic. The von Bertalanffy curve for biological factors represented a plateau similar to an asymptotic quantity, meaning that, above a certain biological energy rate, the bioturbation activity reworks sediment that has already been reworked but without affecting the erodibility of the sediment in old tracks (see Orvain and Sauriau, 2002, for details concerning this mechanism). The curve of eroded material as a function of silt content gradually increased with an increase in silt content. The model showed a slight increase in $Q_{fluff}(t0)$ fitting when the silt content increased in the absence of biota, accounting for a kind of “abiotic fluff layer” comprised of erosion aggregates detached from the bed matrix whose detachment was not caused by macrofaunal activity. The model that only included the biological effect (Supp. Data 2.4.1, Equation 3.1) performed less well (nRMSE = 0.481) than when the sediment factor was included. The dataset by Ciutat_2007 appeared to drive a substantial part of the adjustment, but this effect did not seem to compromise the quality of overall parameterization too much, since, according to a Durbin Watson test (Supp. Data 3.1.1), the data were not affected by any strong autocorrelation.

I.

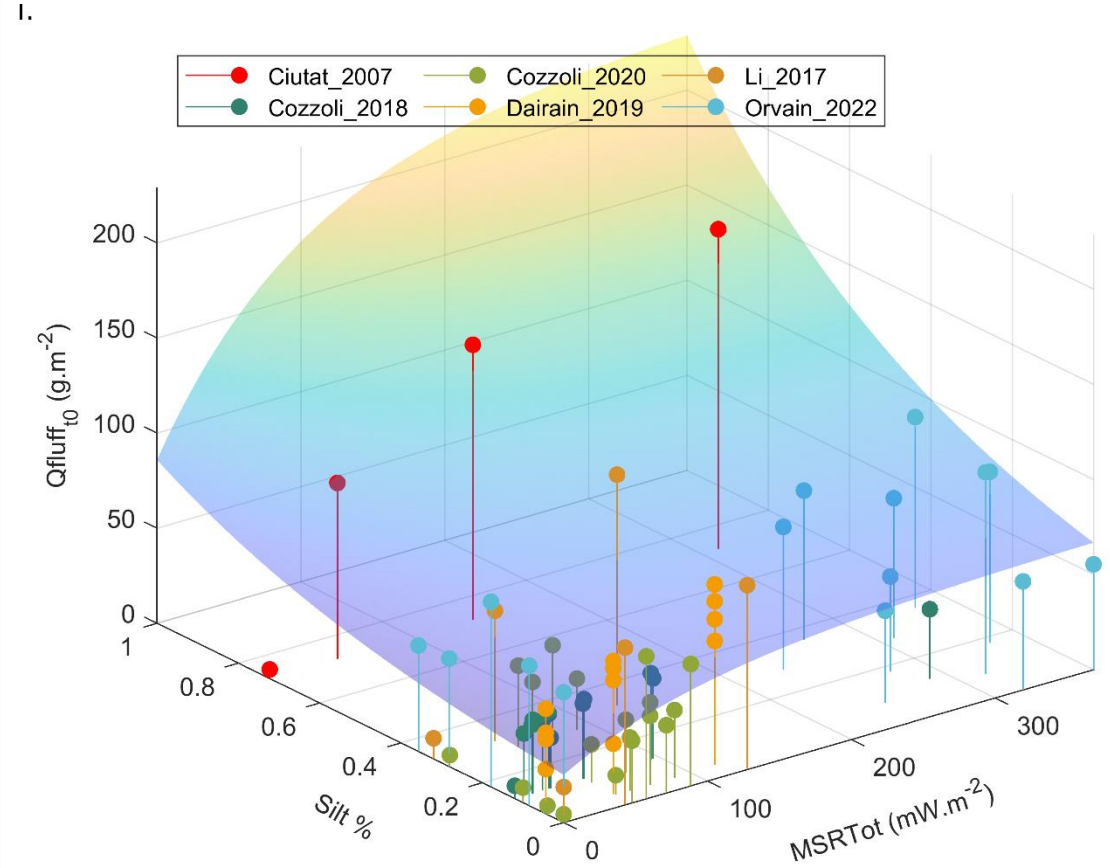

363

364 *Figure 4. Observed Q_{fluff_obs} values for MSRtot (mW.m^{-2}), (%) silt content and its validated $Q_{fluff}(t0)$*
365 *modelled surface.*

366 ### 3.1.2 Abiotic sediment erodibility: control mass erosion (II.)

367 The control set of 58 runs was subdivided into 17 pools each containing one to eight replicates of
368 the same sediment condition (Figure 5, 3D plots in Supp. Fig 3. D, M_{erod} vs time plots in Supp. Fig 3. D).
369 Modelled erosion was satisfactory with a global nRMSE of 0.966 with two parameters:

370 $$E_{mass}(t) = \boldsymbol{E_{0ab}} \cdot \left(\frac{\tau_t}{\boldsymbol{\tau_{mass0ab}}} - 1\right) \; and \; E_{mass} = 0 \; if \; \tau_t < \tau_{mass}$$

371 The Dairain_2019 and Orvain_2022 datasets were the most involved in driving the adjustment
372 process, since they were the runs with the highest BSS (Figure 1). The Cozzoli_2020 dataset was not
373 well simulated, was either under or over-estimated depending on the replicates, but the observed data
374 showed high variability in the same sediment conditions. No particular pattern was observed between
375 the parameters and the silt content (Supp. Fig 3. E), underlining the difficulty of comparing data from
376 different flume experiments. In Cozzoli_2018 and 2020, mass erosion started at the beginning of the
377 run when the BSS was low (respectively $\tau_{mass} = 6.10^{-11}$ and [0.018 to 0.105] Pa).

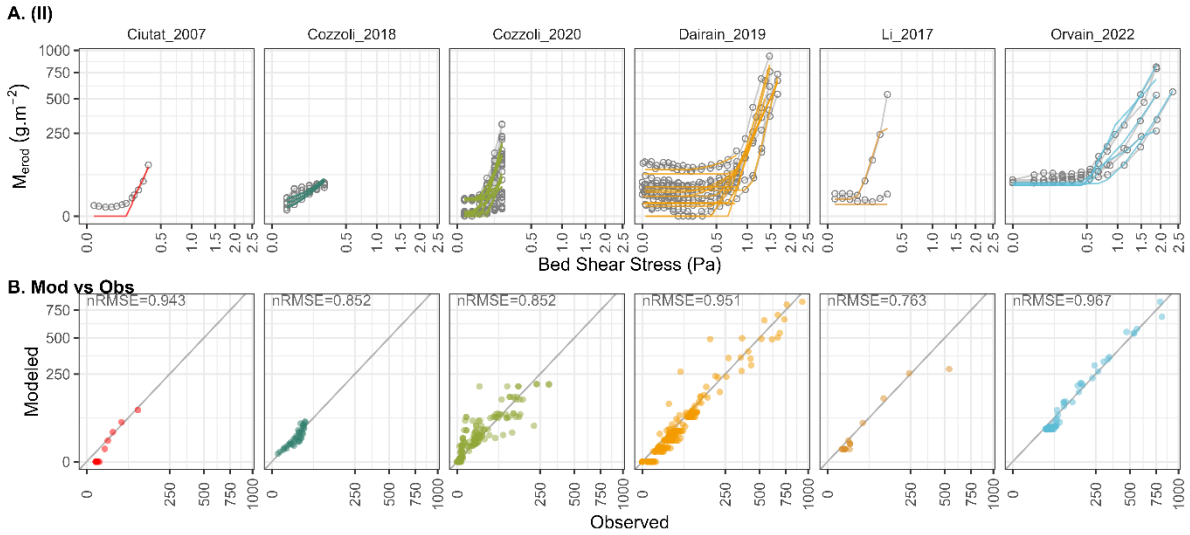

Figure 5. A: Erosion data from control experiments in grey and model II in colours; B: Predicted versus observed data, the grey line represents the 1:1 line. Note that x and y axis are in square root scale.

3.2 Individual fluff & mass erosion (III.)

The grouped datasets were adjusted to the groups of replicates (k=68) using the fluff layer erosion model (Supp. Fig 3.I & L), the mass erosion model (Supp. Fig 3.J & M) and the combined fluff & mass erosion models (Figure 6 & Figure 7 A, Supp. Fig 3.K & N). Although the fluff and mass erosion models were individually efficient (respectively nRMSE = 0.966 and 0.974), the two models combined gave the best fit (nRMSE = 0.981). However, the fluff & mass model required 5 parameters, of which 3 were dedicated to fluff erosion (Q_{fluff} parameters being pre-fitted in I.) and 2 to mass erosion (control parameters E_{0ab} & $\tau_{mass0ab}$ being pre-fitted in II.).

$$E_{fluff}(t) = \boldsymbol{\alpha}.Q_{fluff}(t-dt).\left(\frac{\tau_t}{\boldsymbol{\tau_{fluff}}}-1\right)+\boldsymbol{o}\ and\ E_{fluff}=0\ if\ \tau_t<\tau_{fluff}$$

$$E_{mass}(t) = \boldsymbol{a_{EBio}}.E_{0ab}.\left(\frac{\tau_t}{\boldsymbol{a_{TBio}}.\tau_{mass0ab}}-1\right)\ and\ E_{mass}=0\ if\ \tau_t<\tau_{mass}$$

Specifically, the fluff model performed relatively well in all runs, the best being obtained with the Orvain_2022 dataset, which covered a wide range of silt contents. The mass model performed less well for Cozzoli_2018. Considering the studies individually, both models were generally fit less than the fluff & mass mixed model, which was particularly efficient in simulating the 2-part aspect of the curve (Figure 2). It is noteworthy that, when evaluated visually, mass erosion started sooner than expected, partly due to the $\tau_{mass0ab}$.

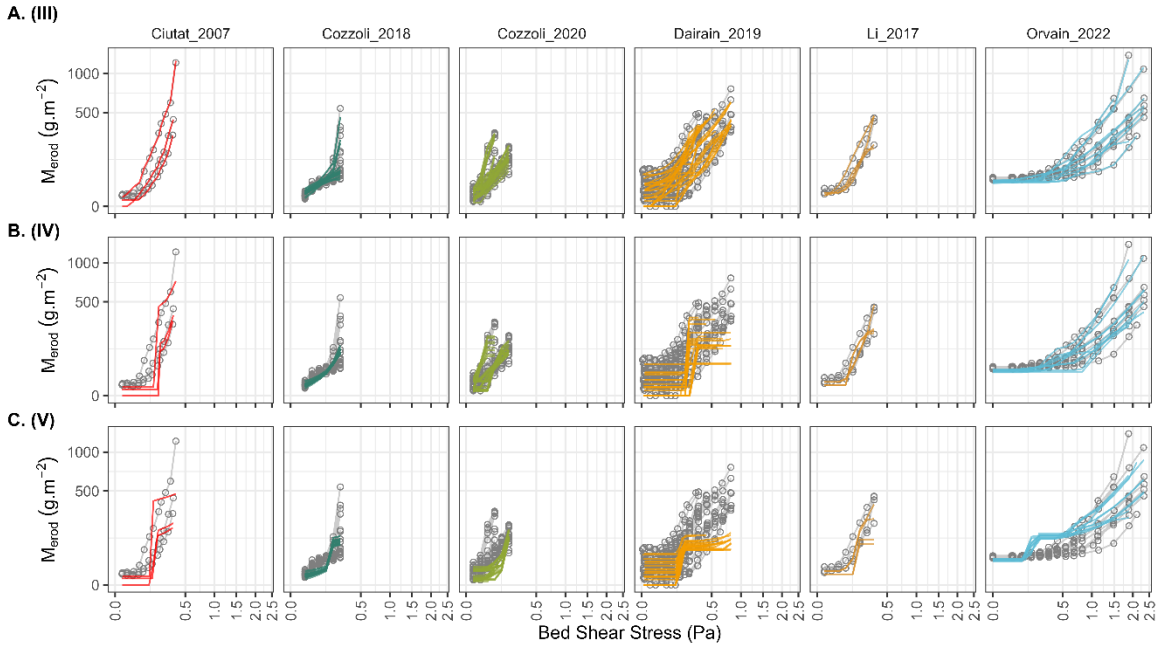

398

399 *Figure 6. Erosion data from data experiments in grey and fluff and mass models in colours,*
400 *respectively A: model III, B: model IV, C: model V. Note that x and y axis are in square root scale. Control*
401 *data are not included for the sake of clarity.*

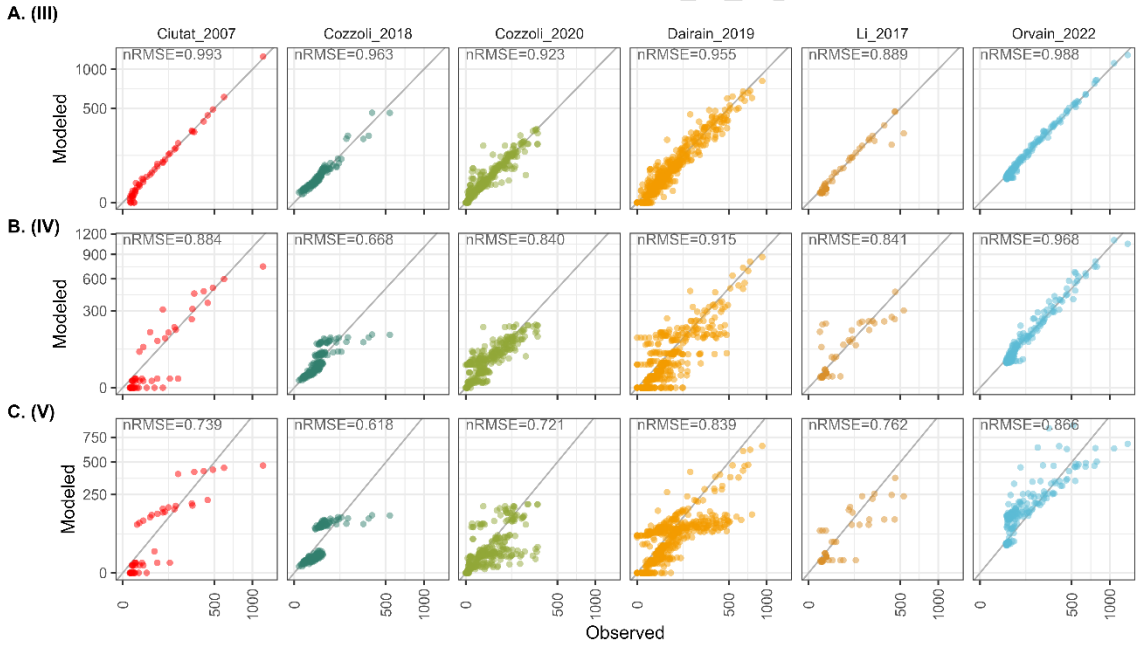

402

403 *Figure 7. Modelled versus observed data, respectively A: model III, B: model IV, C: model V. The*
404 *grey line represents the 1:1 line. Note that x and y axis are in square root scale. Control data are not*
405 *included for the sake of clarity.*

406 ## 3.3 Type of sediment, fluff & mass erosion (IV.)

407 The fluff & mass adjustment was made by pooling data with similar sediment conditions rather than

408 by replicates, the number of different conditions was reduced from 68 to 17 values, the global nRMSE

= 0.957 (Figure 6 & Figure 7 B, Supp. Fig 3.M & S). The model required 7 parameters, of which 3 were dedicated to fluff erosion (Q_{fluff} parameters being pre-fitted in I.) and 4 were used for mass erosion (control parameters E_{0ab} & $\tau_{mass0ab}$ being pre-fitted in II.).

$$E_{fluff}(t) = \boldsymbol{\alpha}.Q_{fluff}(t-dt).\left(\frac{\tau_t}{\boldsymbol{\tau_{fluff}}}-1\right)+\boldsymbol{o}\ and\ E_{fluff}=0\ if\ \tau_t<\tau_{fluff}$$

$$E_{mass}(t) = \boldsymbol{a_{EBio}}.E_{0ab}.\left(\frac{\tau_t}{\tau_{mass0ab}.\left(\boldsymbol{a_{TBio}}.e^{(BioFact.\boldsymbol{b_{TBio}})+\boldsymbol{oo}}\right)}-1\right)\ and\ E_{mass}=0\ if\ \tau_t<\tau_{mass}$$

The general aspect of the model showed a “trigger” effect of erosion, with a too sudden increase in M_{erod}, except in Orvain_2022 and Cozzoli_2018. The Ciutat_2007 dataset showed that the global aspect did not match observations. The $\tau_{mass0ab}$ was low in every run, meaning that even if the modelled fluff and mass erosion equation was used, the solution led to mass erosion starting right at the beginning of the experiment.

3.4 Global fluff & mass adjustment (V.)

The fluff & mass global adjustment was made by pooling all the data, the global nRMSE = 0.911 (Figure 6 & Figure 7 C, Supp. Fig 3. Q & T). The model required 5 parameters, of which 3 were dedicated to fluff erosion (Q_{fluff} parameters being pre-fitted in I.) and 2 were used for mass erosion (control parameters E_{0ab} & $\tau_{mass0ab}$ being pre-fitted in II.).

$$E_{fluff}(t) = \boldsymbol{\alpha}.Q_{fluff}(t-dt).\left(\frac{\tau_t}{\boldsymbol{\tau_{fluff}}}-1\right)+\boldsymbol{o}\ and\ E_{fluff}=0\ if\ \tau_t<\tau_{fluff}$$

$$E_{mass}(t) = \boldsymbol{a_{EBio}}.E_{0ab}.\left(\frac{\tau_t}{\boldsymbol{a_{TBio}}.\tau_{mass0ab}}-1\right)\ and\ E_{mass}=0\ if\ \tau_t<\tau_{mass}$$

Mass erosion started slightly later than in the sediment types, i.e. closer to the observed levels. Except in Orvain_2022 and Li_2017, the M_{erod} level reached a plateau after mass erosion started. The Orvain_2022 study showed a clear fluff sequence before mass erosion. In Dairain_2019, erosion was underestimated, which was also the case in Ciutat_2007.

3.5 Global fluff adjustment (V.): the selected model

The global fluff adjustment was made by pooling all the data and removing all the steps identified as mass erosion steps. The global nRMSE = 0.868 (Figure 8, Supp. Fig 3. V & W). The model required 3 fluff erosion parameters (Q_{fluff} parameters being pre-fitted in I.).

$$Q_{fluff}(t_0) = \left[20.163 \cdot \left(1 - e^{(-0.01.\mathrm{MSRtot})}\right) + 11.837\right] \cdot \left[\left(e^{(1.815.\%Silt)}\right) + 1.12\right]$$

$$E_{fluff}(t) = \mathbf{6.877 \cdot 10^{-6}} \cdot Q_{fluff}(t - dt) \cdot \left(\frac{\tau_t}{\mathbf{0.014}} - 1\right) + \mathbf{0.005} \; and \; E_{fluff} = 0 \; if \; \tau_t < \tau_{fluff}$$

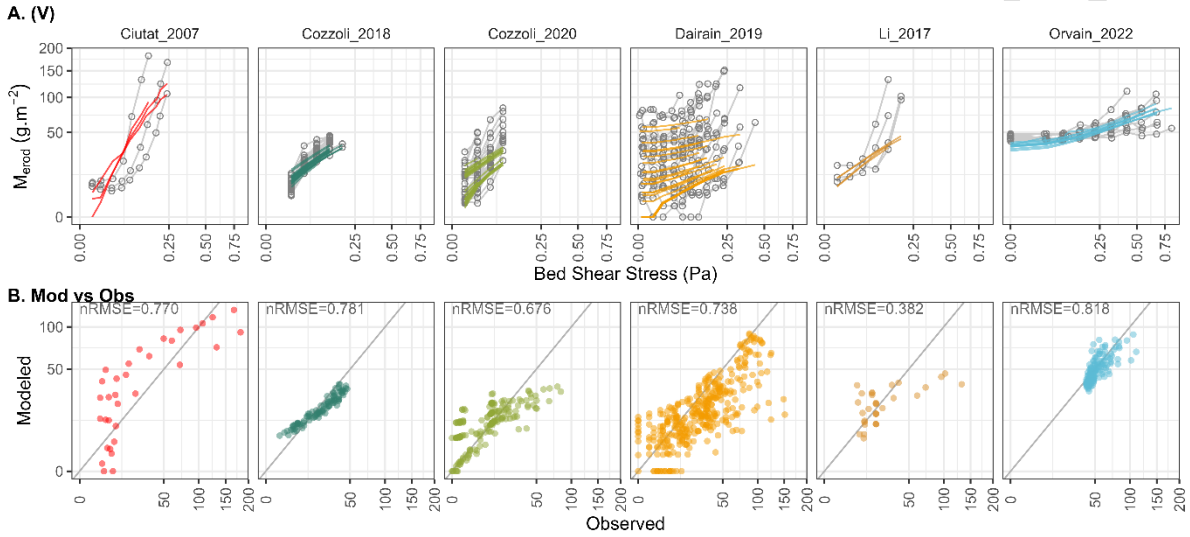

Figure 8. A: Erosion data from data experiments in grey and fluff model V in colours; B: Predicted versus observed data, the grey line represents the 1:1 line. Note that x and y axis are in square root scale. Control data are not included for the sake of clarity.

Table 2: Models validation scores.

Model	Records	AICc	RMSE	nRMSE	df	Parameters	Pools
I. Creation of the fluff layer	68	629	24.281	0.806	5	5	1
II. Abiotic sediment erodibility	28,593	276,580	29.049	0.966	34	2	17
III. Individual fluff erosion	75,581	754,456	34.304	0.966	204	3	68
III. Individual mass erosion	75,581	733,400	29.874	0.974	272	4	68
III. Individual fluff & mass erosion	75,581	703,551	24.557	0.981	476	7	68
IV. Type of sediment, fluff & mass erosion	75,581	729,758	48.230	0.957	153	9	17
V. Global fluff & mass erosion	75,581	883,666	80.136	0.911	5	5	1
V. Global fluff erosion on fluff steps	49,292	419,134	16.583	0.868	3	3	1

3.6 Other parameterization tests

The whole process of this study was designed to obtain - as exhaustively as the technical limits permitted - the most generic model. To this end, model fitting in Matlab was done using Parallel for-Loop (parfor) with the Parallel Computing Toolbox™, which makes it possible to explore several combinations of conditions; a loop on a wide range of initial conditions were set up to ensure the "fminsearch" function found the best minimum. Only relevant results are shown here, but some unsuccessful tests are worth mentioning.

1. The consolidation state of the fluff layer and varying resistance to sediment was accounted for in one test, by allowing the τ_{fluff} and τ_{mass} to evolve with time during the ongoing erosion process (Orvain et al., 2003). To this end, at each time interval, the critical threshold of the sediment was modified according to the quantity of sediment that remained not eroded. The τ_{fluff} equation was tested based on the Q_{fluff} remaining at each *dt* (Supp. Table 3, Equation 7). This addition had the effect of inverting the erosion curve in some runs/steps, revealing an exponential rather than an asymptotic trend. For the τ_{mass}, three equations were based on the total amount of eroded sediment (because there is no 'remaining' quantity), with the possibility of having different curve shapes (Supp. Table 3, Equation 8). One seemed rather promising when adjusting the control runs, but increased the complexity of adjusting the biological runs.
2. To deal with the sediment variability, a global adjustment of control runs was made by adjusting E0 and τ_{mass} using the silt content (Supp. Table 3, Equations 9 and 10). The silt content was the sediment factor chosen because it was the only factor present in all the datasets we collected. In the combination of equations (Supp. Table 3, Equation 8 was not included), the model was only able to fit the ERIS datasets (Orvain_2022 and Dairain_2017), while the other simulations showed no mass erosion at all.
3. In order to limit the number of parameters adjusted simultaneously and to manage differences in magnitude between fluff and mass erosion, the global fluff model was used as a source of input parameters for the global mass erosion adjustment. However, with the exception of the Orvain_2022 dataset, the model showed no mass erosion.

4. The fluff model was tested without the alpha parameter, which could be considered as buffering the parameterized Q_{fluff}. However, the result was a complete failure.
5. All processes were tested with density (ind.m^{-2}) and biomass (g.m^{-2}) as BioFact. Density was systematically less adequate than the other, the biomass being equivalent in results than the MSRTot, mainly due to the narrow range of temperatures in the dataset, even though MSRTot showed a global best performance.

4 Discussion

4.1 What the modelling process revealed

Individual erosion adjustments are useful to evaluate the performance of different types of models (fluff layer, sediment mass and their combination), removing the experimental dispersion that could jeopardise the model readings. The model that simulated mass erosion performed well, along with the model that simulated fluff layer erosion alone; however, the version that mixed fluff layer and mass erosion was clearly the most reliable. Although improving the model by mixing the two processes requires more parameters, doing so makes it possible to distinguish the two processes and give more applicability to different measurement conditions (Orvain, 2005; Orvain et al., 2003). In fact, the two processes are based on equations with different profiles (Figure 2), and the observed profiles can only be rendered by combining them, as long as the experiment reaches a sufficiently high BSS.

The choice of using the metabolic rate in this type of exercise, over and above its interest in describing bioturbation processes in the context of the Metabolic Theory of Ecology (Brown et al., 2004), is that it allows different experimental designs to be combined. Indeed, the different sample surfaces are an important driver in the choice of the size and number of individuals installed. As (Cozzoli et al., 2020) showed, density and biomass information alone are not sufficient to describe the effect of bioturbation of the cockle on the sediment. In addition, the measurements were taken at different temperatures, which, although within a fairly low range (12 to 18°C), can have an effect on the activity of the individuals in the sample. With a view to modelling in extrapolated temperature ranges, while remaining within the tolerance range of the species, it is possible with the metabolic rate to take account of these variations in activity, which may be reflected in sediment reworking.

The individual fluff & mass models used the adjustment of $Q_{fluff}(t0)$, an estimate of the quantity of sediment reworked by the fauna. As the observation of this quantity of sediment was indirect and rather empirical, the performance obtained was fairly good. This estimate uses two generic descriptors that are interesting from a biological point of view. On the one hand, the type of sediment is known to have an impact on the bioturbatory activity of *C. edule*, as well as on many species of benthic macrofauna, and silt content is known to be a good indicator of this (Carss et al., 2020). On the other hand, the metabolic rate can express bioturbation as an energy flow transmitted to the sediment, which enables comparisons between the effects of individuals with different body sizes and potentially different species. The development of the model by Cozzoli et al (Cozzoli et al., 2018) concerning $Q_{fluff}(t0)$, did not take any dependency on the composition of the sediment into consideration, but was a linear function of the faunal factor (i.e. the metabolic rate). That kind of relation cannot account for a well-known process: the surface saturation effect, the fauna at some point reworking the same sediment, hence the choice of a von Bertalanffy relationship (Orvain and Sauriau, 2002). The quality of the model that simulates erosion of the fluff layer could still be improved by collecting more data, paying particular attention to the intermediate values in the range of the chosen factors. The same model would also benefit from a less indirect method of measurement, such as topographic measurement of the reworked sediment from a smoothed surface, to estimate the volume of the fluff layer more precisely and to reinforce the process-based approach. This bioturbation model (and not erosion) is the first step towards the construction of a community-scale bioturbation model that uses the metabolic rate to describe surficial bioturbation effects and sediment-water column interactions (Maire et al., 2008).

The models that simulated fluff layer and sediment mass erosion were also based on adjustments made on control data, which gave significantly different parameters for Equation 4. We did not find a satisfactory solution when we applied the mass erosion equation globally, even when we attempted to include a silt content dependence function. This result means that the silt content was not an appropriate descriptor to define the erodibility of the sediment prepared in these flume studies. In fact, the description of sediment features requires numerous parameters (particle size distribution, water content, sediment density) and their vertical distribution, information which is not systematically collected during flume experiments. Moreover, the procedure used to prepare the sediment also considerably modifies sediment characteristics such as the state of consolidation and its vertical structure. For instance, the experiment conducted by (Ciutat et al., 2007) was designed to maintain the natural state and stratified

layers of the natural field sediments to the greatest possible extent, whereas the other experiments included major modifications, such as defaunation, mixing, sieving and removal of biofilm, and the sediment was introduced into the flume by letting it decant in water (Cozzoli et al., 2020, 2018; Li et al., 2017) or moulded in a container (Dairain et al., 2020b).

However, as it stands, the individual fluff & mass model cannot be used to describe bioturbation and erosion processes. The generalisation of the model via the adjustment by sediment conditions only allowed us to focus on biological factors. The model that combined all the sediment conditions led to a diminishing performance, but the reduction in the degree of freedom was significant (from 408 to 136) for only two additional parameters. The performance of the Dairain_2019 dataset was poor during fitting of the model, which must be due to the fact that the biological parasitism factor was clearly responsible for reduced bioturbation activity. For now, such information could not be included in the model, because it was not available in the other papers.

The global fluff & mass parameterization was undertaken based on the hypotheses that 1) adjustment of the control sediment conditions accounted for all sediment and flume variability, 2) the biological factors were satisfactorily described by the metabolic rate. The model performance diminished, but with a massive reduction of degree of freedom (from 136 to 7). Nevertheless, the model failed to satisfactorily describe erosion over time, its success varied with the dataset, and still used the control parameters (vector of length 17) as inputs. This model is thus not sufficiently global nor sufficiently efficient to be considered fully generic and reliable in diverse HMS models and estuaries.

Our final proposal is a global model, without mass erosion, developed by combining the creation of a surficial fluff layer (the Q_{fluff} model) and its erosion. The Q_{fluff} model is a new insight as it accounts for the metabolic activity of the species studied *C. edule*, and its response to the type of sediment using a meta-analysis approach. In previous *C. edule* model studies, only fauna density indices or sediment factors were considered (Dairain et al., 2020b; Rakotomalala et al., 2015). The model developed by (Cozzoli et al., 2019) includes a metabolic rate approach, model sediment resuspension versus the metabolic rate and the BSS, but does not adjust the erosion pattern kinetics (and especially the effect of time *dt*). As the biological effect had already been described, erosion of the fluff layer was then simple and robust to fit globally at the scale of the meta-analysis. This model was designed to be introduced in an HMS model to refine the modelling of sediment transport, with the conversion of biomass and density to MSR via Allen's equation (Allen et al., 2005). With that aim in view, the combination of fluff and mass

processes also appears to be mandatory to be sure all the biological effects are properly incorporated in sediment transport models.

4.2 A recommendation for improving flume experiments

Problems with the general adjustment of bioturbation and fauna effect on erodibility are mainly encountered in the case of cohesive sediments. Sand erosion is less complex to model, and requires fewer parameters to describe. On the other hand, cohesive and mixed sediments are intrinsically complex to characterise. It is thus necessary to work on bioturbation issues, taking care to describe the sediment used as precisely as possible. Working in collaboration with sedimentology scientists would also ensure factors or parameters that could be decisive in terms of model development are not neglected (Grabowski et al., 2011; Le Hir et al., 2011; Mitchener and Torfs, 1996; Tolhurst et al., 2005).

When measuring the effects of bioturbation, the practice to measure the control immediately before measuring the biological sample, and to use the control to keep only the biological effect, like in the study by (Cozzoli et al., 2020), appears to be very efficient. However, this is technically impossible in the case of one-way flumes like ERIS, for which the same sediment bed cannot be redeposited to be experimented twice.

Measuring the actual BSS requires further study. Flume calibration is generally performed on a smooth surface, but this does not account for the autogenous roughness effects of the individuals present on the sample (Friedrichs et al., 2000). As soon as the cockle scratches the surface of the sediment, it modifies the hydraulic conditions, and hence BSS. In fact, the degree of roughness does not remain the same over the course of the flume experiment, but changes throughout the erosion ongoing process, all the more so as a bioturbator fauna is present (Dairain et al., 2020b). The ERIS is equipped for upstream/downstream measurement of the pressure in the flume, enabling the difference in pressure to be used to measure a 'rough' BSS that is more representative of dynamic reality. What is more, BSS calibration does not account for variations in the height of the water column during erosion, which can vary unchecked when the flume is driven by the upper surface of the water. When only the fluff layer is involved, these effects can be considered negligible, but this remains to be proven when mass erosion is involved. In addition, the autogenic bioturbation effects are not taken into account in a annular flume built nowadays (Dombroski and Crimaldi, 2007).

585 The choice of flume equipment is also decisive. The annular flume is efficient for fluff erosion, but
586 cannot be used to investigate mass erosion. The ERIS flume can handle both types of erosion, thanks
587 to its powerful pump, but there are many experimental biases, especially because of the small size of
588 the sediment sample. It would be useful to perform experiments that more closely resemble the kinetics
589 of annular flume experiments, with fewer but longer steps, to observe a clearer equilibrium. CSMs
590 (Tolhurst et al., 1999), for example, are better designed for mass erosion than other devices. Inter-
591 calibration of the different methods is necessary, and in the meantime, accurate distinction of the two
592 types of erosion is not possible. We need to better define whether it is possible to observe both types of
593 erosion in a single experiment (Tolhurst et al., 2000; Vardy et al., 2007; Widdows et al., 2007).

594 In addition, the flumes used in these experiments are of two types, both of which are unidirectional,
595 among a wide possibilities of flumes, either in lab or in-situ (Tolhurst et al., 2009). There are also
596 oscillation channels, or wave channels, which more closely reproduce the complex hydrodynamic
597 conditions and turbulence field that could occur in the field. Examples include wave mesocosms
598 (Infantes et al., 2021), wave channel for *in-situ* or lab cores (de Smit et al., 2021), and portable channel
599 for in-situ measurements (de Smit et al., 2020). Comparative measurements between the two types
600 show that the results are not equivalent depending on the type of instrument used (Jepsen et al., 2004,
601 2012), thus preventing pooling data from unidirectional and oscillatory flumes.

602 Some flumes make it possible to use sediment taken directly *in-situ* (as in (Ciutat et al., 2007)),
603 keeping its natural structure, which makes erodimetry measurements more realistic. It is also possible
604 to carry out *in situ* measurements directly using flume designed for this purpose. However, in this case,
605 the biological parameters are less well controlled, which makes modelling more complex. Most
606 laboratory prepared sediment are highly altered, but clarify the results depending on biological factor,
607 which are still delicate to analyse. To our knowledge, no comparative study has been carried out to
608 assess the difference in results using the same sediment in its natural state and defaunated and
609 prepared in the laboratory.

610 The procedure for preparing the samples also needs to be more clearly defined. Indeed, depending
611 on the objective of the experiment, attention needs to be paid to different factors: the sediment
612 preparation method as mentioned above, but also the fauna bioturbation phase. If we consider the
613 genesis of the fluff layer, the time spent by the fauna on the sample and its history are both crucial as is
614 accurate biometric measurement of all individuals. Knowledge of a tidal rhythm, the temperature of the

615 environment, and the duration of bioturbation, as distinct from the duration of settlement or even
616 acclimatation, is also essential when defining the Q_{fluff}. If bioturbation lasts long enough or if the density
617 of fauna is high enough to reach saturation of the reworked surface before measurement, it is no longer
618 possible to assess the mediation of sediment erodibility by biological organisms. On the other hand, the
619 activities of many animals differ radically depending on the moment of the tide. Consequently, it is
620 necessary to define bioturbation activity during alternating daily fluctuations with immersion and
621 emersion phases. The cockle has a wide range of individual behaviours including filtering with open
622 siphons, burial when the current becomes too strong. The fluff layer involves a direct bioresuspension
623 process for cockles with an immediate effect linked to valve movements at the surface, and cockles are
624 less active at low tide. The fluff layer produced by cockles is completely different from the fluff layer
625 (mainly tracks) created by the model gastropod *Peringia ulvae* species, for which the first models of the
626 fluff layer were developed during emersed periods (Orvain et al., 2003), providing alternate phases in
627 long term simulations (Orvain et al., 2012): (i) emersion periods showing accumulation of the quantity
628 of sediment in the fluff layer over time and (ii) immersion periods with a potential reduction in the quantity
629 of sediment because the animals do not crawl when they are covered in water and the resuspension
630 rate and bed shear stress are high enough.

631 In addition, treatment of the sediment and the condition of the mesocosm can affect the presence or
632 absence of microphytobenthos (MPB), which has a role in the bioturbation process (Andersen et al.,
633 2010; Dairain et al., 2020b; Orvain et al., 2004). On one hand, MPB form biofilm made of
634 exopolysaccharides (EPS) which reinforces cohesiveness and/or reduces the roughness of the
635 sediment surface, which can limit erosion (Andersen et al., 2010; Sutherland et al., 1998). On the other
636 hand, MPB is a source of food for different species, in particular *C. edule*, which can cause resuspension
637 of sediment through its efforts to access MPB (Rakotomalala et al., 2015).

638 Further, when the metabolic rate is used rather than historical descriptors, experimental temperature
639 becomes a factor that needs to be controlled, and even studied as a dedicated factor to be thoroughly
640 investigated. Indeed, if we assume that bioturbatory activity is linked – among other things – to the basal
641 activity of the individual and hence to temperature, then for the same pool of individuals, Q_{fluff} must vary
642 with variations in temperature. In the present study, temperature was not a factor, and it was not possible
643 to compare the temperatures of the different datasets, as the biomasses were not equivalent. Having
644 said that, further research is required to explore the effect of temperature and its influence on

bioturbation and related processes, and many questions require close collaboration with specialists in the metabolism of benthic fauna. Taking temperature into account is also useful when considering the seasonality of benthic macrofauna activities. Biomass and population density vary significantly throughout the year, but so does their metabolism. How do these factors influence bioturbation activity over the course of a year?

5 Conclusion

The aim of this study was to propose a sediment erosion model including *Cerastoderma edule* bioturbation. The first step was to develop a model for the creation of the biogenic (fluff) layer linked to cockle bioturbation activity. However, it was not possible to combine the processes of fluff layer erosion and mass erosion in a single generic model. We therefore propose a model that focusses only on erosion of the fluff layer, but incorporates creation of the fluff layer model as a function of the metabolic rate and silt content. We provide a general model for measurements made using different equipment, under a wide range of conditions. The model is therefore a first step in the process-based modelling of fluff erosion. In addition, the use of the metabolic rate means that temperature can be incorporated in the model, enabling questions of bioturbation activity to be developed over the course of the seasons, not only from a demographic point of view, but also in terms of physiological status.

ACKNOWLEDGEMENTS

The authors are grateful to the following researchers who gave permission to use their data: Aurélie Ciutat, Francesco Cozzoli, Tjeerd Bouma and Baoquan Li.

The authors acknowledge anonymous reviewers for their valuable comments and suggestions.

FUNDING

This research was supported by the *Region Normandie* (A. Lehuen's PhD) and by the *Office Français pour la Biodiversité* (the MELTING POTES project).

CREDIT AUTHOR STATEMENT

A. Lehuen: Conceptualisation, Methodology, Formal analysis, Writing - Original Draft, Funding acquisition; **F. Orvain**: Conceptualisation, Methodology, Validation, Formal analysis, Resources, Writing - Reviewing & Editing, Supervision, Project administration, Funding acquisition

References

Akaike, H., 1974. A new look at the statistical model identification. IEEE Trans. Autom. Control 19, 716–723. https://doi.org/10.1109/TAC.1974.1100705

Allen, A.P., Gillooly, J.F., Brown, J.H., 2005. Linking the global carbon cycle to individual metabolism. Funct. Ecol. 19, 202–213. https://doi.org/10.1111/j.1365-2435.2005.00952.x

Amos, C.L., Daborn, G.R., Christian, H.A., Atkinson, A., Robertson, A., 1992. In situ erosion measurements on fine-grained sediments from the Bay of Fundy. Mar. Geol. 108, 175–196. https://doi.org/10.1016/0025-3227(92)90171-D

Andersen, T.J., 2001. Seasonal Variation in Erodibility of Two Temperate, Microtidal Mudflats. Estuar. Coast. Shelf Sci. 53, 1–12. https://doi.org/10.1006/ecss.2001.0790

Andersen, T.J., Jensen, K.T., Lund-Hansen, L., Mouritsen, K.N., Pejrup, M., 2002. Enhanced erodibility of fine-grained marine sediments by Hydrobia ulvae. J. Sea Res. 48, 51–58. https://doi.org/10.1016/S1385-1101(02)00130-2

Andersen, T.J., Lanuru, M., Van Bernem, C., Pejrup, M., Riethmueller, R., 2010. Erodibility of a mixed mudflat dominated by microphytobenthos and Cerastoderma edule, East Frisian Wadden Sea, Germany. Estuar. Coast. Shelf Sci., Mechanisms of sediment retention in estuaries 87, 197–206. https://doi.org/10.1016/j.ecss.2009.10.014

Baas, J.H., Davies, A.G., Malarkey, J., 2013. Bedform development in mixed sand–mud: The contrasting role of cohesive forces in flow and bed. Geomorphology 182, 19–32. https://doi.org/10.1016/j.geomorph.2012.10.025

Barbier, E.B., Hacker, S.D., Kennedy, C., Koch, E.W., Stier, A.C., Silliman, B.R., 2011. The value of estuarine and coastal ecosystem services. Ecol. Monogr. 81, 169–193. https://doi.org/10.1890/10-1510.1

Brey, T., 2010. An empirical model for estimating aquatic invertebrate respiration: Aquatic invertebrate respiration. Methods Ecol. Evol. 1, 92–101. https://doi.org/10.1111/j.2041-210X.2009.00008.x

Brey, T., Müller-Wiegmann, C., Zittier, Z.M.C., Hagen, W., 2010. Body composition in aquatic organisms — A global data bank of relationships between mass, elemental composition and energy content. J. Sea Res. 64, 334–340. https://doi.org/10.1016/j.seares.2010.05.002

Brown, J.H., Gillooly, J.F., Allen, A.P., Savage, V.M., West, G.B., 2004. Toward a metabolic theory of ecology. Ecology 85, 1771–1789. https://doi.org/10.1890/03-9000

Carss, D.N., Brito, A.C., Chainho, P., Ciutat, A., de Montaudouin, X., Fernández Otero, R.M., Filgueira, M.I., Garbutt, A., Goedknegt, M.A., Lynch, S.A., Mahony, K.E., Maire, O., Malham, S.K., Orvain, F., van der Schatte Olivier, A., Jones, L., 2020. Ecosystem services provided by a non-cultured shellfish species: The common cockle Cerastoderma edule. Mar. Environ. Res. 158, 104931. https://doi.org/10.1016/j.marenvres.2020.104931

Ciutat, A., Widdows, J., Pope, N.D., 2007. Effect of Cerastoderma edule density on near-bed hydrodynamics and stability of cohesive muddy sediments. J. Exp. Mar. Biol. Ecol. 346, 114–126. https://doi.org/10.1016/j.jembe.2007.03.005

Cozzoli, F., Bouma, T.J., Ottolander, P., Lluch, M.S., Ysebaert, T., Herman, P.M.J., 2018. The combined influence of body size and density on cohesive sediment resuspension by bioturbators. Sci. Rep. 8, 3831. https://doi.org/10.1038/s41598-018-22190-3

Cozzoli, F., Eelkema, M., Bouma, T.J., Ysebaert, T., Escaravage, V., Herman, P.M.J., 2014. A Mixed Modeling Approach to Predict the Effect of Environmental Modification on Species Distributions. PLoS ONE 9, e89131. https://doi.org/10.1371/journal.pone.0089131

Cozzoli, F., Gjoni, V., Del Pasqua, M., Hu, Z., Ysebaert, T., Herman, P.M.J., Bouma, T.J., 2019. A process based model of cohesive sediment resuspension under bioturbators' influence. Sci. Total Environ. 670, 18–30. https://doi.org/10.1016/j.scitotenv.2019.03.085

Cozzoli, F., Gomes da Conceição, T., Van Dalen, J., Fang, X., Gjoni, V., Herman, P.M.J., Hu, Z., Soissons, L.M., Walles, B., Ysebaert, T., Bouma, T.J., 2020. Biological and physical drivers of bio-mediated sediment resuspension: A flume study on Cerastoderma edule. Estuar. Coast. Shelf Sci. 241, 106824. https://doi.org/10.1016/j.ecss.2020.106824

Dairain, A., Maire, O., Meynard, G., Orvain, F., 2020a. Does parasitism influence sediment stability? Evaluation of trait-mediated effects of the trematode Bucephalus minimus on the key role of cockles Cerastoderma edule in sediment erosion dynamics. Sci. Total Environ. 733, 139307. https://doi.org/10.1016/j.scitotenv.2020.139307

Dairain, A., Maire, O., Meynard, G., Richard, A., Rodolfo-Damiano, T., Orvain, F., 2020b. Sediment stability: can we disentangle the effect of bioturbating species on sediment erodibility from their impact on sediment roughness? Mar. Environ. Res. 162, 105147. https://doi.org/10.1016/j.marenvres.2020.105147

de Smit, J.C., Kleinhans, M.G., Gerkema, T., Bouma, T.J., 2021. Quantifying natural sediment erodibility using a mobile oscillatory flow channel. Estuar. Coast. Shelf Sci. 262, 107574. https://doi.org/10.1016/j.ecss.2021.107574

de Smit, J.C., Kleinhans, M.G., Gerkema, T., Timmermans, K.R., Bouma, T.J., 2020. Introducing the TiDyWAVE field flume: A method to quantify natural ecosystem resilience against future storm waves. Limnol. Oceanogr. Methods 18, 585–598. https://doi.org/10.1002/lom3.10386

Degraer, S., Wittoeck, J., Appeltans, W., Cooreman, K., Deprez, T., Hillewaert, H., Hostens, K., Mees, J., Vanden Berghe, E., Vincx, M., 2006. The Macrobenthos Atlas of the Belgian Part of the North Sea.

D'Errico, J., 2006. fminsearchbnd, fminsearchcon [WWW Document]. MATLAB Cent. File Exch. URL https://fr.mathworks.com/matlabcentral/fileexchange/8277-fminsearchbnd-fminsearchcon (accessed 8.18.23).

Diaz, M., Grasso, F., Hir, P.L., Sottolichio, A., Caillaud, M., Thouvenin, B., 2020. Modeling Mud and Sand Transfers Between a Macrotidal Estuary and the Continental Shelf: Influence of the Sediment Transport Parameterization. J. Geophys. Res. Oceans 125, e2019JC015643. https://doi.org/10.1029/2019JC015643

Dombroski, D.E., Crimaldi, J.P., 2007. The accuracy of acoustic Doppler velocimetry measurements in turbulent boundary layer flows over a smooth bed. Limnol. Oceanogr. Methods 5, 23–33. https://doi.org/10.4319/lom.2007.5.23

Donadi, S., van der Zee, E.M., van der Heide, T., Weerman, E.J., Piersma, T., van de Koppel, J., Olff, H., Bartelds, M., van Gerwen, I., Eriksson, B.K., 2014. The bivalve loop: Intra-specific facilitation in burrowing cockles through habitat modification. J. Exp. Mar. Biol. Ecol. 461, 44–52. https://doi.org/10.1016/j.jembe.2014.07.019

Dronkers, J., van den Berg, J., 2023. Coastal and marine sediments [WWW Document]. Coastalwiki. URL http://www.coastalwiki.org/wiki/Coastal_and_marine_sediments (accessed 8.18.23).

Eriksson, B.K., Westra, J., van Gerwen, I., Weerman, E., van der Zee, E., van der Heide, T., van de Koppel, J., Olff, H., Piersma, T., Donadi, S., 2017. Facilitation by ecosystem engineers enhances nutrient effects in an intertidal system. Ecosphere 8, e02051. https://doi.org/10.1002/ecs2.2051

Friedrichs, M., Graf, G., Springer, B., 2000. Skimming flow induced over a simulated polychaete tube lawn at low population densities. Mar. Ecol. Prog. Ser. 192, 219–228. https://doi.org/10.3354/meps192219

Grabowski, R.C., Droppo, I.G., Wharton, G., 2011. Erodibility of cohesive sediment: The importance of sediment properties. Earth-Sci. Rev. 105, 101–120. https://doi.org/10.1016/j.earscirev.2011.01.008

Grasso, F., Le Hir, P., Bassoullet, P., 2015. Numerical modelling of mixed-sediment consolidation. Ocean Dyn. 65, 607–616. https://doi.org/10.1007/s10236-015-0818-x

Harris, R., Pilditch, C., Hewitt, J., Lohrer, A., Van Colen, C., Townsend, M., Thrush, S., 2015. Biotic interactions influence sediment erodibility on wave-exposed sandflats. Mar. Ecol. Prog. Ser. 523, 15–30. https://doi.org/10.3354/meps11164

Hayward, P.J., Ryland, J.S., 1995. Handbook of the marine fauna of north-west Europe. Oxford University Press.

Herman, P.M.J., Middelburg, J.J., Heip, C.H.R., 2001. Benthic community structure and sediment processes on an intertidal flat: results from the ECOFLAT project. Cont. Shelf Res., European Land-Ocean Interaction 21, 2055–2071. https://doi.org/10.1016/S0278-4343(01)00042-5

Herman, P.M.J., Middelburg, J.J., Van De Koppel, J., Heip, C.H.R., 1999. Ecology of Estuarine Macrobenthos, in: Nedwell, D.B., Raffaelli, D.G. (Eds.), Advances in Ecological Research, Estuaries. Academic Press, pp. 195–240. https://doi.org/10.1016/S0065-2504(08)60194-4

Infantes, E., de Smit, J.C., Tamarit, E., Bouma, T.J., 2021. Making realistic wave climates in low-cost wave mesocosms: A new tool for experimental ecology and biogeomorphology. Limnol. Oceanogr. Methods 19, 317–330. https://doi.org/10.1002/lom3.10425

Jepsen, R., Roberts, J., Gailani, J., 2004. Erosion Measurements in Linear, Oscillatory, and Combined Oscillatory and Linear Flow Regimes. J. Coast. Res. 20, 1096–1101. https://doi.org/10.2112/03-0003R.1

Jepsen, R.A., Roberts, J.D., Kearney, S.P., Dimiduk, T.G., O'Hern, T.J., Gailani, J.Z., 2012. Shear Stress Measurements and Erosion Implications for Wave and Combined Wave-Current Generated Flows. J. Waterw. Port Coast. Ocean Eng. 138, 323–329. https://doi.org/10.1061/(ASCE)WW.1943-5460.0000137

Joensuu, M., Pilditch, C.A., Harris, R., Hietanen, S., Pettersson, H., Norkko, A., 2018. Sediment properties, biota, and local habitat structure explain variation in the erodibility of coastal sediments: Variation in the erodibility of coastal sediments. Limnol. Oceanogr. 63, 173–186. https://doi.org/10.1002/lno.10622

Jones, C.G., Lawton, J.H., Shachak, M., 1994. Organisms as Ecosystem Engineers. Oikos 69, 373–386. https://doi.org/10.2307/3545850

Le Hir, P., Cayocca, F., Waeles, B., 2011. Dynamics of sand and mud mixtures: A multiprocess-based modelling strategy. Cont. Shelf Res., Proceedings of the 9th International Conference on Nearshore and Estuarine Cohesive Sediment Transport Processes 31, S135–S149. https://doi.org/10.1016/j.csr.2010.12.009

Le Hir, P., Monbet, Y., Orvain, F., 2007. Sediment erodability in sediment transport modelling: Can we account for biota effects? Cont. Shelf Res., Natural Coastal Mechanisms - Flume and Field Experiments on Links between Biology, Sediments and Flow 27, 1116–1142. https://doi.org/10.1016/j.csr.2005.11.016

Li, B., Cozzoli, F., Soissons, L.M., Bouma, T.J., Chen, L., 2017. Effects of bioturbation on the erodibility of cohesive versus non-cohesive sediments along a current-velocity gradient: A case study on cockles. J. Exp. Mar. Biol. Ecol. 496, 84–90. https://doi.org/10.1016/j.jembe.2017.08.002

Li, J., Chen, X., Townend, I., Shi, B., Du, J., Gao, J., Chuai, X., Gong, Z., Wang, Y.P., 2021. A comparison study on the sediment flocculation process between a bare tidal flat and a clam aquaculture mudflat: The important role of sediment concentration and biological processes. Mar. Geol. 434, 106443. https://doi.org/10.1016/j.margeo.2021.106443

Maire, O., Lecroart, P., Meysman, F., Rosenberg, R., Duchêne, J., Grémare, A., 2008. Quantification of sediment reworking rates in bioturbation research: a review. Aquat. Biol. 2, 219–238. https://doi.org/10.3354/ab00053

Mitchener, H., Torfs, H., 1996. Erosion of mud/sand mixtures. Coast. Eng. 29, 1–25. https://doi.org/10.1016/S0378-3839(96)00002-6

Needham, H.R., Pilditch, C.A., Lohrer, A.M., Thrush, S.F., 2013. Density and habitat dependent effects of crab burrows on sediment erodibility. J. Sea Res. 76, 94–104. https://doi.org/10.1016/j.seares.2012.12.004

Orvain, F., 2005. A model of sediment transport under the influence of surface bioturbation: generalisation to the facultative suspension-feeder Scrobicularia plana. Mar. Ecol. Prog. Ser. 286, 43–56. https://doi.org/10.3354/meps286043

Orvain, F., Hir, P.L., Sauriau, P.-G., 2003. A model of fluff layer erosion and subsequent bed erosion in the presence of the bioturbator, <I>Hydrobia ulvae</I>. J. Mar. Res. 61, 821–849. https://doi.org/10.1357/002224003322981165

824 Orvain, F., Le Hir, P., Sauriau, P.-G., Lefebvre, S., 2012. Modelling the effects of macrofauna on
825 sediment transport and bed elevation: Application over a cross-shore mudflat profile and model
826 validation. Estuar. Coast. Shelf Sci., ECSA 46 Conference Proceedings 108, 64–75.
827 https://doi.org/10.1016/j.ecss.2011.12.036

828 Orvain, F., Sauriau, P., Sygut, A., Joassard, L., Le Hir, P., 2004. Interacting effects of Hydrobia ulvae
829 bioturbation and microphytobenthos on the erodibility of mudflat sediments. Mar. Ecol. Prog.
830 Ser. 278, 205–223. https://doi.org/10.3354/meps278205

831 Orvain, F., Sauriau, P.-G., 2002. Environmental and behavioural factors affecting activity in the intertidal
832 gastropod Hydrobia ulvae. J. Exp. Mar. Biol. Ecol. 272, 191–216. https://doi.org/10.1016/S0022-
833 0981(02)00130-2

834 Orvain, F., Sauriau, P.-G., Le Hir, P., Guillou, G., Cann, P., Paillard, M., 2007. Spatio-temporal variations
835 in intertidal mudflat erodability: Marennes-Oléron Bay, western France. Cont. Shelf Res. 27,
836 1153–1173. https://doi.org/10.1016/j.csr.2006.05.013

837 Paarlberg, A.J., Knaapen, M.A.F., de Vries, M.B., Hulscher, S.J.M.H., Wang, Z.B., 2005. Biological
838 influences on morphology and bed composition of an intertidal flat. Estuar. Coast. Shelf Sci. 64,
839 577–590. https://doi.org/10.1016/j.ecss.2005.04.008

840 Partheniades, E., 1965. Erosion and Deposition of Cohesive Soils. J. Hydraul. Div. 91, 105–139.
841 https://doi.org/10.1061/JYCEAJ.0001165

842 Rakotomalala, C., Grangeré, K., Ubertini, M., Forêt, M., Orvain, F., 2015. Modelling the effect of
843 Cerastoderma edule bioturbation on microphytobenthos resuspension towards the planktonic
844 food web of estuarine ecosystem. Ecol. Model. 316, 155–167.
845 https://doi.org/10.1016/j.ecolmodel.2015.08.010

846 Sanchez, A., 2006. digitize [WWW Document]. MATLAB Cent. File Exch. URL
847 https://fr.mathworks.com/matlabcentral/fileexchange/8139-digitize (accessed 8.18.23).

848 Seibel, B.A., Drazen, J.C., 2007. The rate of metabolism in marine animals: environmental constraints,
849 ecological demands and energetic opportunities. Philos. Trans. R. Soc. B Biol. Sci. 362, 2061–
850 2078. https://doi.org/10.1098/rstb.2007.2101

851 Shi, B., Pratolongo, P.D., Du, Y., Li, J., Yang, S.L., Wu, J., Xu, K., Wang, Y.P., 2020. Influence of
852 Macrobenthos (Meretrix meretrix Linnaeus) on Erosion-Accretion Processes in Intertidal Flats:
853 A Case Study From a Cultivation Zone. J. Geophys. Res. Biogeosciences 125,
854 e2019JG005345. https://doi.org/10.1029/2019JG005345

855 Soissons, L.M., Gomes da Conceiçâo, T., Bastiaan, J., van Dalen, J., Ysebaert, T., Herman, P.M.J.,
856 Cozzoli, F., Bouma, T.J., 2019. Sandification vs. muddification of tidal flats by benthic
857 organisms: A flume study. Estuar. Coast. Shelf Sci. 228, 106355.
858 https://doi.org/10.1016/j.ecss.2019.106355

859 Sutherland, T.F., Grant, J., Amos, C.L., 1998. The effect of carbohydrate production by the diatom
860 Nitzschia curvilineata on the erodibility of sediment. Limnol. Oceanogr. 43, 65–72.
861 https://doi.org/10.4319/lo.1998.43.1.0065

862 Thrush, S., Hewitt, J., Herman, P., Ysebaert, T., 2005. Multi-scale analysis of species-environment
863 relationships. Mar. Ecol.-Prog. Ser. 302, 13–26. https://doi.org/10.3354/Meps302013

864 Tolhurst, T.J., Black, K.S., Paterson, D.M., 2009. Muddy Sediment Erosion: Insights from Field Studies.
865 J. Hydraul. Eng. 135, 73–87. https://doi.org/10.1061/(ASCE)0733-9429(2009)135:2(73)

866 Tolhurst, T.J., Black, K.S., Paterson, D.M., Mitchener, H.J., Termaat, G.R., Shayler, S.A., 2000. A
867 comparison and measurement standardisation of four in situ devices for determining the erosion
868 shear stress of intertidal sediments. Cont. Shelf Res. 20, 1397–1418.
869 https://doi.org/10.1016/S0278-4343(00)00029-7

870 Tolhurst, T.J., Black, K.S., Shayler, S.A., Mather, S., Black, I., Baker, K., Paterson, D.M., 1999.
871 Measuring the in situ Erosion Shear Stress of Intertidal Sediments with the Cohesive Strength
872 Meter (CSM). Estuar. Coast. Shelf Sci. 49, 281–294. https://doi.org/10.1006/ecss.1999.0512

873 Tolhurst, T.J., Underwood, A.J., Perkins, R.G., Chapman, M.G., 2005. Content versus concentration:
874 Effects of units on measuring the biogeochemical properties of soft sediments. Estuar. Coast.
875 Shelf Sci. 63, 665–673. https://doi.org/10.1016/j.ecss.2005.01.010

876 Ubertini, M., Lefebvre, S., Gangnery, A., Grangeré, K., Le Gendre, R., Orvain, F., 2012. Spatial
877 Variability of Benthic-Pelagic Coupling in an Estuary Ecosystem: Consequences for
878 Microphytobenthos Resuspension Phenomenon. PLoS ONE 7, e44155.
879 https://doi.org/10.1371/journal.pone.0044155

880 Ubertini, M., Lefebvre, S., Rakotomalala, C., Orvain, F., 2015. Impact of sediment grain-size and biofilm
881 age on epipelic microphytobenthos resuspension. J. Exp. Mar. Biol. Ecol. 467, 52–64.
882 https://doi.org/10.1016/j.jembe.2015.02.007

883 van Prooijen, B.C., Montserrat, F., Herman, P.M.J., 2011. A process-based model for erosion of
884 Macoma balthica-affected mud beds. Cont. Shelf Res. 31, 527–538.
885 https://doi.org/10.1016/j.csr.2010.12.008

886 Vardy, S., Saunders, J.E., Tolhurst, T.J., Davies, P.A., Paterson, D.M., 2007. Calibration of the high-
887 pressure cohesive strength meter (CSM). Cont. Shelf Res. 27, 1190–1199.
888 https://doi.org/10.1016/j.csr.2006.01.022

889 Widdows, J., Brinsley, M., 2002. Impact of biotic and abiotic processes on sediment dynamics and the
890 consequences to the structure and functioning of the intertidal zone. J. Sea Res., Structuring
891 Factors of Shallow Marine Coastal Communities, Part I 48, 143–156.
892 https://doi.org/10.1016/S1385-1101(02)00148-X

893 Widdows, J., Brinsley, M.D., Bowley, N., Barrett, C., 1998. A Benthic Annular Flume for In Situ
894 Measurement of Suspension Feeding/Biodeposition Rates and Erosion Potential of Intertidal
895 Cohesive Sediments. Estuar. Coast. Shelf Sci. 46, 27–38.
896 https://doi.org/10.1006/ecss.1997.0259

897 Widdows, J., Friend, P.L., Bale, A.J., Brinsley, M.D., Pope, N.D., Thompson, C.E.L., 2007. Inter-
898 comparison between five devices for determining erodability of intertidal sediments. Cont. Shelf
899 Res. 27, 1174–1189. https://doi.org/10.1016/j.csr.2005.10.006

900 Willows, R.I., Widdows, J., Wood, R.G., 1998. Influence of an infaunal bivalve on the erosion of an
901 intertidal cohesive sediment: A flume and modeling study. Limnol. Oceanogr. 43, 1332–1343.
902 https://doi.org/10.4319/lo.1998.43.6.1332

903 Wood, R., Widdows, J., 2002. A model of sediment transport over an intertidal transect, comparing the
904 influences of biological and physical factors. Limnol. Oceanogr. 47, 848–855.
905 https://doi.org/10.4319/lo.2002.47.3.0848

906 Ysebaert, T., Herman, P.M.J., 2002. Spatial and temporal variation in benthic macrofauna and
907 relationships with environmental variables in an estuarine, intertidal soft-sediment environment.
908 Mar. Ecol. Prog. Ser. 244, 105–124. https://doi.org/10.3354/meps244105

909 Zhou, Z., Bouma, T.J., Fivash, G.S., Ysebaert, T., van IJzerloo, L., van Dalen, J., van Dam, B., Walles,
910 B., 2022. Thermal stress affects bioturbators' burrowing behavior: A mesocosm experiment on
911 common cockles (Cerastoderma edule). Sci. Total Environ. 824, 153621.
912 https://doi.org/10.1016/j.scitotenv.2022.153621

913

914

Reference list

Figure 1. A: Bed sheer stress (BSS [Pa]) time scheme for each experiment, B: Resuspended mass (M_{erod} [$g.m^{-2}$]) versus time for each experiment and C: the metabolic rate calculated (MSRTot [$mW.m^{-2}$]) versus the sediment silt content [%] for each experiment.

Figure 2. Sketch of erosion processes in the fluff layer erosion (green line), mass erosion (solid red line) and the parameters used. The dashed black line represents the addition of the two processes, the M_{erod} measured in the experiment. The straight dashed black line represents the linear regression of the mass erosion steps that determined the critical mass erosion threshold (τ_{mass} [Pa]).

Figure 3. Scheme of the adjustments made, p is the number of parameters, k the number of sub-groups, and df represents the degree of freedom as p*k.

Figure 4. Observed Q_{fluff_obs} values for MSRtot ($mW.m^{-2}$), (%) silt content and its validated $Q_{fluff}(t0)$ modelled surface.

Figure 5. A: Erosion data from control experiments in grey and model II in colours; B: Predicted versus observed data, the grey line represents the 1:1 line. Note that x and y axis are in square root scale.

Figure 6. Erosion data from data experiments in grey and fluff and mass models in colours, respectively A: model III, B: model IV, C: model V. Note that x and y axis are in square root scale. Control data are not included for the sake of clarity.

Figure 7. Predicted versus observed data, respectively A: model III, B: model IV, C: model V. The grey line represents the 1:1 line. Note that x and y axis are in square root scale. Control data are not included for the sake of clarity.

Figure 8. A: Erosion data from data experiments in grey and fluff model V in colours; B: Predicted versus observed data, the grey line represents the 1:1 line. Note that x and y axis are in square root scale. Control data are not included for the sake of clarity.

940 # Table list

943